

DESIGN AND DEVELOPMENT OF AN INDUCTIVE POWER TRANSFER SYSTEM FOR CHARGING OF BATTERY IN WRIST WATCHES WITH METALLIC BACK PLATE

A Project Report

submitted by

ANISH BABU

*in partial fulfilment of the requirements
for the award of the degree of*

MASTER OF TECHNOLOGY



**DEPARTMENT OF ELECTRICAL ENGINEERING
INDIAN INSTITUTE OF TECHNOLOGY MADRAS.**

MAY 2014

THESIS CERTIFICATE

This is to certify that the thesis titled **DESIGN AND DEVELOPMENT OF AN INDUCTIVE POWER TRANSFER SYSTEM FOR CHARGING OF BATTERY IN WRIST WATCHES WITH METALLIC BACK PLATE**, submitted by **ANISH BABU**, to the Indian Institute of Technology, Madras, for the award of the degree of **Master of Technology**, is a bona fide record of the research work done by him under our supervision. The contents of this thesis, in full or in parts, have not been submitted to any other Institute or University for the award of any degree or diploma.

Dr. Bobby George
Research Guide
Assistant Professor
Dept. of Electrical Engineering
IIT-Madras, 600 036

Place: Chennai
Date: 12th May 2014

ACKNOWLEDGEMENTS

It gives me great pleasure in expressing my sincere and heartfelt gratitude to my project guide Dr. Bobby George for his excellent guidance, motivation and constant support throughout my project. I consider myself extremely fortunate to have had a chance to work under his supervision. It has been a very learning and enjoyable experience to work under him.

I would like to thank TITAN Industries Ltd for providing the necessary watches and components for testing the charging system.

My appreciation to my fellow research scholars in the Measurements and Instrumentation Laboratory, especially Anoop, Arjun and Piyush for spending their invaluable time with me, in discussing about the project and answering my queries, goes well beyond words. I would also extend my thanks to Anand, Biswarup, Supriya and Prashanth for their support during my work.

Last but not the least, I would like to thank my parents and family for their support and the Almighty for uncountable blessings due to which I was able to complete the project on time.

ABSTRACT

KEYWORDS: Inductive Power Transfer; Smart Watch; Receiver Detection; Wireless battery charging; loosely coupled transformer.

Modern smart watches have high energy requirements and needs to be recharged regularly. The preference for water resistant watches in the market rules out direct charging through a charging port. A contact less watch battery charging system using inductive power transfer (IPT) method is proposed in this thesis.

Wireless battery charging modules currently available for mobile phones and similar gadgets packaged in a non-conductive casing are not suitable for wrist watches with conductive back plate. The high frequency magnetic field generated to transfer power cannot pass through the conductive back plate. The limited space inside the watch cannot accommodate all the components needed to establish a communication link between the charger and the receiver. No non-contact charging system is currently available for wrist watches with metallic back plate.

The proposed system operate at a frequency well below the limit set by skin effect. The developed can charge batteries of various voltage levels like 3.6 V, 3 V, 2.3 V and 1.5 V. It can detect the presence of an IPT enabled watch when it is kept on top of it and start charging. It will automatically stop charging once the watch is removed from the charger or when the watch battery is fully charged. It can also detect the type of battery inside the watch and charge it accordingly. All this is achieved with minimal extra components inside the watch. A prototype system has been developed and tested, It can transmit power at a maximum efficiency of 35.2%. The currently available systems for low power transmission upto 5 Watts through non metallic surfaces has efficiency close to 60%.

TABLE OF CONTENTS

ACKNOWLEDGEMENTS	i
ABSTRACT	ii
LIST OF TABLES	v
LIST OF FIGURES	vii
ABBREVIATIONS	viii
NOTATION	ix
1 INTRODUCTION	1
1.1 Wireless Power Transmission	2
1.2 Equivalent Mathematical Model	2
1.3 Battery Charging Profile	5
1.4 Organization of Thesis	6
2 DESIGN OF THE IPT SYSTEM	7
2.1 Basic Schematic	7
2.2 Magnetic Circuit Design	9
2.2.1 Transmitter core	10
2.2.2 Receiver Core	11
2.2.3 Coil Parameters	13
2.3 Transmitter Circuit Design	13
2.4 Receiver Circuit Design	14
2.5 Selection of Charging Frequency	17
3 CHARGER FEATURES AND ITS IMPLEMENTATION	20
3.1 Introduction	20
3.2 Watch Detection	20

3.3	Watch Removal Detection	21
3.4	Charge Complete Detection	22
3.5	Battery Type Detection	23
3.6	Charging Algorithm	26
4	RESULTS AND EVALUATION	28
4.1	Results	28
4.2	Efficiency Analysis	31
4.2.1	Core loss measurement	33
4.2.2	Separation of core loss	33
4.2.3	Efficiency under loaded conditions	34
4.3	Coefficient of Coupling k	35
5	CONCLUSION AND FUTURE WORK	36
5.1	Conclusion	36
5.2	Future Scope	37
A	PCB LAYOUTS	38

LIST OF TABLES

2.1	Transmitter and Receiver coil parameters.	13
4.1	No load test for separation of core losses.	34
4.2	Efficiency under different load conditions	35

LIST OF FIGURES

1.1	Wireless charger for mobile phones	2
1.2	Wireless power transmitter module	3
1.3	Wireless charging system	3
1.4	Equivalent circuit	4
1.5	Primary circuit with the reflected impedance Z_r	4
1.6	Charge profile of a 2.3 V battery	5
1.7	Charge profile of 3.6 V battery	6
2.1	(a) Top view and (b) Side view of the charger unit with watch	7
2.2	Basic schematic diagram of the IPT system	8
2.3	Magnetic Circuit (Side View).	9
2.4	Top View of the receiver.	9
2.5	Flux density in the core.	10
2.6	(a) shows the 'L' and 'I' pieces forming the 'U' shaped core. (b) shows the individual piece dimensions. All dimensions in mm	11
2.7	Transmitter core dimensions	11
2.8	Bobbin Dimensions. (a) Front view, (b) Side view and (c) Top view. All dimensions in mm	12
2.9	(a) shows the 'I' shaped pieces forming the 'U' shaped core. (b) shows the individual piece dimensions. All dimensions in mm	12
2.10	Receiver core dimensions. (a) Front view and (b) Side view. All dimensions in mm	12
2.11	Transmitter and receiver coils developed	13
2.12	Transmitter and receiver circuit schematic diagram.	15
2.13	Complete Transmitter circuit.	16
2.14	Transmitter circuit fabricated on PCB.	17
2.15	Receiver circuit for 3.6 V battery.	18
2.16	Receiver circuit for 3 V battery.	18
2.17	Receiver circuit fabricated on PCB and fixed inside the watch.	18

3.1	Bode plot of v_c with and without C_s	21
3.2	ϕ_1, ϕ_2, v_c and v_g with and without C_s	22
3.3	Bode plot of v_c with and without the watch on the charger.	23
3.4	ϕ_1, ϕ_2, v_c and v_g with and without the watch on the charger.	24
3.5	Phase measured by MCU	25
3.6	Bode plot of v_c with S_5 on and off.	25
3.7	Charging algorithm flowchart	27
4.1	Test setup showing the prototyping board, power supply, micro controller and the excitation and control circuits	28
4.2	v_c and v_g during search mode when C_s is not connected across the receiver coil L_s	29
4.3	v_c and v_g during search mode when an IPT enabled watch is kept on charger.	29
4.4	v_c and v_g during charging mode when an IPT enabled watch is kept on the charger.	29
4.5	v_c and v_g during charging mode when the watch is removed from the charger.	30
4.6	v_c and v_g during charging mode when watch battery is fully charged.	30
4.7	The comparator output, and the switching pulse ϕ_2 which are given as input to the AND gate and its output v_g plotted in that order when the watch is being charged	31
4.8	The non overlapping switching pulses ϕ_1 and ϕ_2 generated by the MCU. They drive the MOSFET H-bridge which powers the primary coil.	31
4.9	The IPT enabled watch kept on the charger developed.	32
4.10	Receiver circuit with an LED connected at its output to show its operation receiving power from the charger	32
A.1	Transmitter PCB layout	38
A.2	Receiver PCB layout	39

ABBREVIATIONS

IPT	Inductive Power Transfer
SWG	Standard Wire Gauge
MCU	Micro controller
IC	Integrated Circuit
PCB	Printed Circuit Board

NOTATION

L_p	Primary coil
L_s	Secondary coil
M	Mutual inductance between primary and secondary coil
k	Coefficient of coupling between primary and secondary coil
C_p	Primary capacitance
C_s	Secondary capacitance
R_p	Primary coil resistance
R_s	Secondary coil resistance
C_{s1}	Capacitance in series with switch S_5
C_{FL}	Secondary filter capacitance
V_{CH}	Charging voltage
V_D	Detection voltage
f_{CH}	Charging frequency
f_D	Detection frequency
v_c	Voltage at the node between L_p and C_p
v_g	Voltage at output of the AND gate
ϕ_1, ϕ_2	Complimentary switching pulses generated by MCU
V_{L_p}	Voltage across L_p
I_{L_p}	Current through L_p
P_{in}	Input Power to the IPT charger
P_{out}	Output Power across the load
P_{copper}	Total Copper loss
P_{core}	Total Core loss
P_e	Power loss due to eddy current
P_h	Power loss due to hysteresis

CHAPTER 1

INTRODUCTION

Smart watches with added features like health monitoring, music player etc. have increased energy requirement, demanding the watch battery used, to be recharged on a regular basis. Direct charging (like in a mobile phone) of the watch battery requires a charging port, to make direct electrical contacts with the battery circuit. This is not viable in water-resistant/tight watches, which are preferred in the market. Therefore, contact less/wireless transfer of power [1],[2] to the rechargeable battery inside the watch is a choice.

Although wireless battery charging modules are available [3] - [6] for mobile phones and similar gadgets packaged in a non-conductive casing, they are not suited for wrist watch with conductive (metallic) back plate/cover. These transmit power through magnetic fields at high frequencies typically in the range of 100 kHz and above. Due to skin effect, these fields cannot pass through the metallic back plate. So the charger has to be operated at a lower frequency. To induce the same voltage in the receiver coil, we will now have to increase the number of turns in the coil which increases the size of the coil. This coil along with the associated circuitry for rectification and for communication between the charger and the receiver will not fit within the limited space available inside the watch.

When a conductive plate is present in the magnetic path of IPT, excitation at super low frequencies (e.g., 50 Hz) has been proposed in [7] for applications within closed metal walls. At such frequencies skin effect does not come in to play. But the magnetic field required to induce the required input voltage will be very high as the number of turns in the receiver is limited by space constraints inside the watch and this can disturb the operation of the watch.

The proposed system operate at a much higher frequency which is within the limits set by skin effect. A suitable magnetic path is provided to guide the magnetic field away from the watch movement. The receiver circuit is designed to fit within a diameter of 20 mm with a thickness of 2.3 mm. The charger can detect the presence of an IPT enabled

watch and will start charging only when it detects one. It stops charging once the watch is removed from the charger and when the watch battery is fully charged. This ensures that no magnetic field is produced around the charger when watch is not present and also a low idle state power consumption. It is also able to detect the type of battery inside the watch. The battery can either be a low power battery with capacity in the range of 10 mA-h or a high power battery with capacity in the range of 150 mA-h and above. Both have different charging requirements and must be charged accordingly.

1.1 Wireless Power Transmission

Today wireless charging is available for a variety of devices. The amount of power that is to be transmitted varies from 5 Watt (for mobile phones) to several kilo Watts (for electric cars). Fig 1.1 shows a mobile phone kept on a wireless charging pad. The power requirement of a smart watch is comparable to that of the mobile phone. The transmitter is kept inside the charger and is powered by a 19 V adapter. The receiver coil and the associated circuits are kept inside the mobile phone near its back cover and the power is transmitted through the plastic case.

A low power wireless power transmission module is shown in Fig 1.2. These can be used for charging mobile phone batteries connected to a suitable receiver circuit. They can transmit power in the range of 5 W through non conductive surfaces.



Figure 1.1: Wireless charger for mobile phones [8]

1.2 Equivalent Mathematical Model

A simplified wireless charging system is shown in fig 1.3. The transmitter and receiver coil are inductively coupled. Coupling factor is usually low for these systems. The transmitter coil is excited by a voltage source which produces a magnetic field, a part

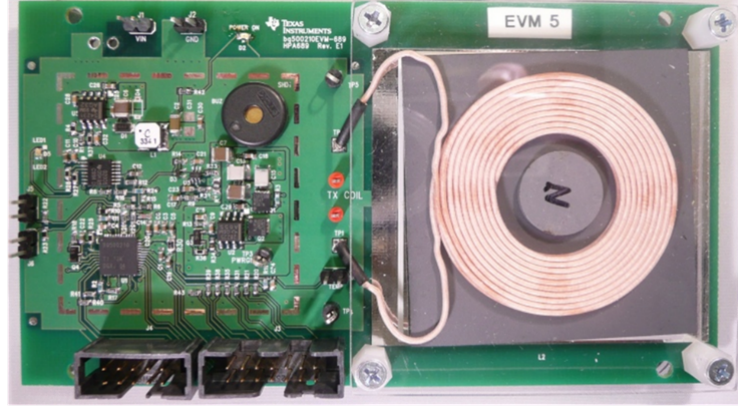


Figure 1.2: A low power wireless transmitter module for transmitting power up to 5 W. The planar transmitter coil and the excitation and control circuits can be seen. [9]

of which links the secondary coil and induces a voltage in the receiver. The equivalent circuit of the contact less transformer is shown in Fig 1.4 as given by [10]. L_p and L_s are the primary and secondary winding with resistances R_p and R_s respectively. Series capacitance C_s improves the power factor as seen from the driving circuit. A parallel capacitor C_s is added in the secondary side and this topology is referred to as series compensated primary and parallel compensated secondary (SP) in [11]. The secondary side can be represented as a reflected impedance in the primary side as shown in Fig 1.5.

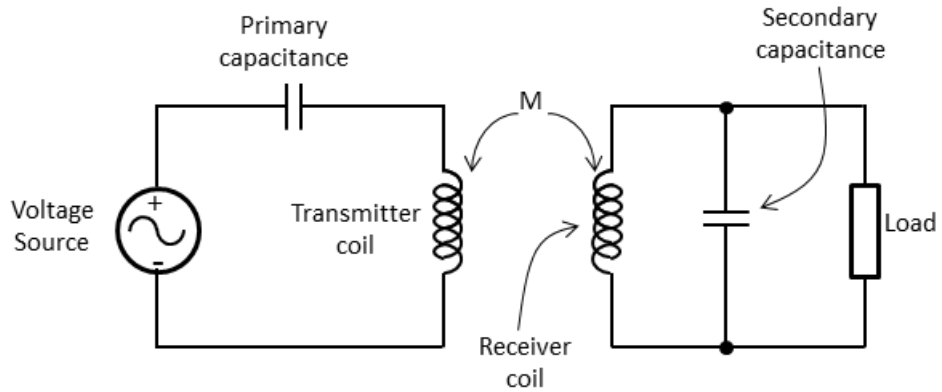


Figure 1.3: Wireless charging system

The reflected impedance Z_r is given by (1.1). Here M is the mutual inductance, ω the input frequency and R_L the load resistance. The input active power is dissipated across the primary coil winding resistance R_p and ReZ_r . The power across ReZ_r is transferred to the secondary where a part of it is dissipated across the secondary coil

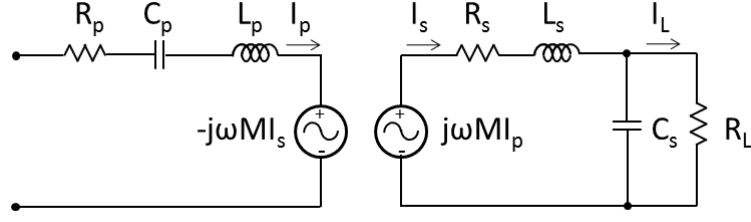


Figure 1.4: Equivalent circuit

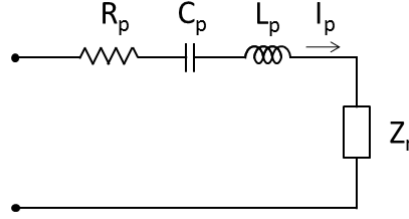


Figure 1.5: Primary circuit with the reflected impedance Z_r

winding resistance R_s and remaining across the load [10]. The maximum power transfer to the secondary side using minimum input VA occurs when $\omega^2 C_s L_s$ is unity.

$$ReZ_r = \frac{\omega^2 M^2 R_L}{R_L^2 (\omega^2 C_s L_s - 1) + \omega^2 L_s^2} \quad (1.1)$$

$$ImZ_r = \frac{-\omega^3 M^2 [C_s R_L^2 (\omega^2 C_s L_s - 1) + L_s]}{R_L^2 (\omega^2 C_s L_s - 1) + \omega^2 L_s^2}$$

When the transformer is excited at this frequency, the secondary side is in resonance and the current through the coil is high. To allow this current, thick copper wires have to be used. The maximum frequency with which power can be transferred to the receiver side is limited by skin effect of the conductive watch back plate and therefore to induce the required voltage in the receiver the number of turns have to be increased. The space available inside the watch is small and hence it is not possible to use coil made of thick copper wire with large number of turns. So to reduce the coil current and thereby the copper wire thickness the charging frequency is kept below the secondary resonant frequency. This secondary resonant frequency is used for watch detection which is discussed in detail in chapter 3.

The overall efficiency of the contact less transformer is given by $\eta = \eta_p \eta_s$, where η_p

is the efficiency of the primary side and η_s the efficiency of the secondary side given by (1.2). The primary side efficiency can be increased by increasing ReZ_r (by keeping $\omega^2 C_s L_s$ as close to one as possible) and by reducing R_s . The secondary side efficiency depends on the R_L and is high for low values of R_L .

$$\eta_p = \frac{ReZ_r}{ReZ_r + R_p} \quad (1.2)$$

$$\eta_s = \frac{R_L}{R_L + R_s + R_s R_L^2 \omega^2 C_s^2}$$

1.3 Battery Charging Profile

The low capacity low voltage batteries and the 3.6 V batteries have completely different charging profile. The charging current of the 2.3 V battery comes down very quickly and is below 0.5 mA for most of the charging period. From a fully discharged state the battery can be charged to a reasonable level in 5 hours. The 3.6 V Lithium ion battery is charged at constant current for some time after which it is charged at constant voltage. A battery management IC is used to charge the 3.6 V battery and it can automatically switch from the constant current mode to constant voltage mode. The charging profile is shown in Fig 1.6 and 1.7.

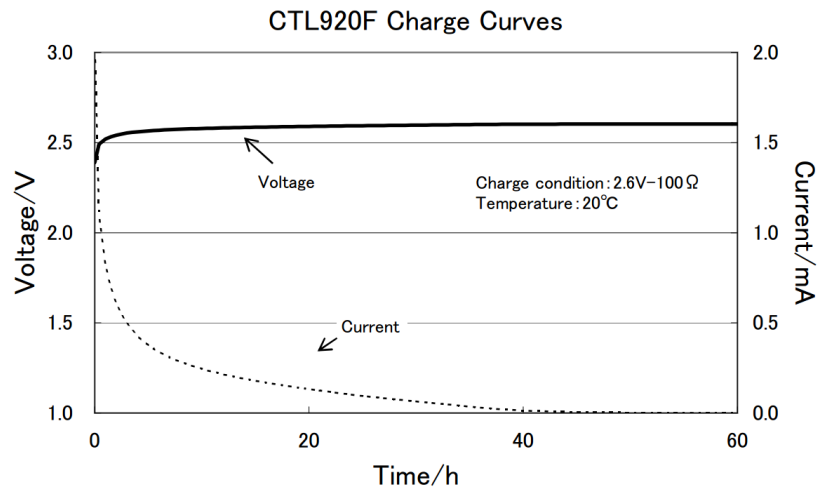


Figure 1.6: Charge profile of a 2.3 V battery [12]

The secondary side efficiency of the transformer depends on the load current and it reduces as the current decreases. The efficiency can be very low while charging the 1.5

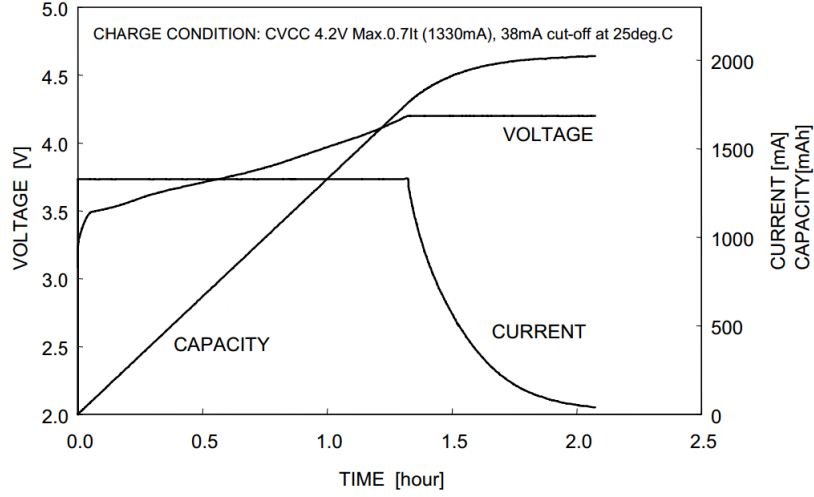


Figure 1.7: Charge profile of 3.6 V battery [12]

V, 2.3 V or the 3 V batteries.

1.4 Organization of Thesis

Chapter 1 gives a brief introduction about the scope and objectives of this project. The equivalent mathematical model and the charging profile of batteries is discussed. In the second chapter, the design of the magnetic circuit including the core and the winding details are given. The transmitter and receiver circuit designs and the circuit diagrams are also given.

In chapter 3, the implementation of the various features of the proposed IPT charger are presented. In chapter 4, a detailed study of the efficiency of the system under different conditions is given. The actual waveforms observed during watch detection, removal and charging completion are also presented.

In chapter 5, the conclusion and scope for future work is presented.

CHAPTER 2

DESIGN OF THE IPT SYSTEM

2.1 Basic Schematic

The watch to be charged has to be placed on the charger as shown in Fig.2.1. The charging unit has a primary coil which is magnetically coupled to the secondary coil of the receiver unit kept inside the watch as shown in Fig.2.2.

When the primary coil is excited from a suitable source, there will be magnetic field lines coupled with the secondary coil as in a transformer and power will be transferred to the receiver coil, which is connected to the battery with suitable electronic modules. The power required for the exciter unit will be taken from the supply mains (230 V, 50 Hz) followed by an AC to DC converter. The charger unit has an exciter circuitry and a measurement and control unit. The receiver unit with required winding, magnetic parts and electronic unit for rectification and voltage regulation and charging control are arranged in a single module and kept inside the watch.

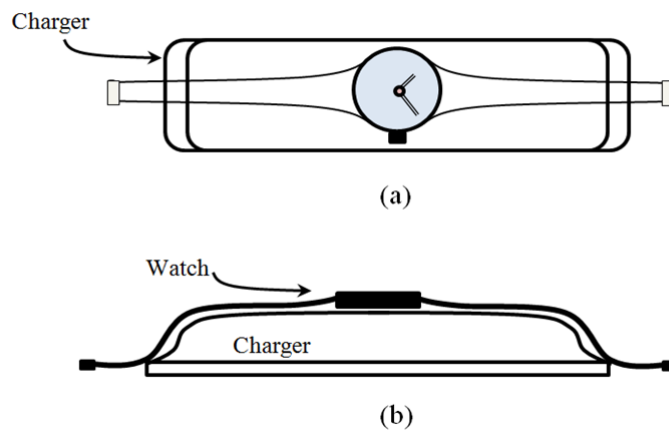


Figure 2.1: (a) Top view and (b) Side view of the charger unit with watch

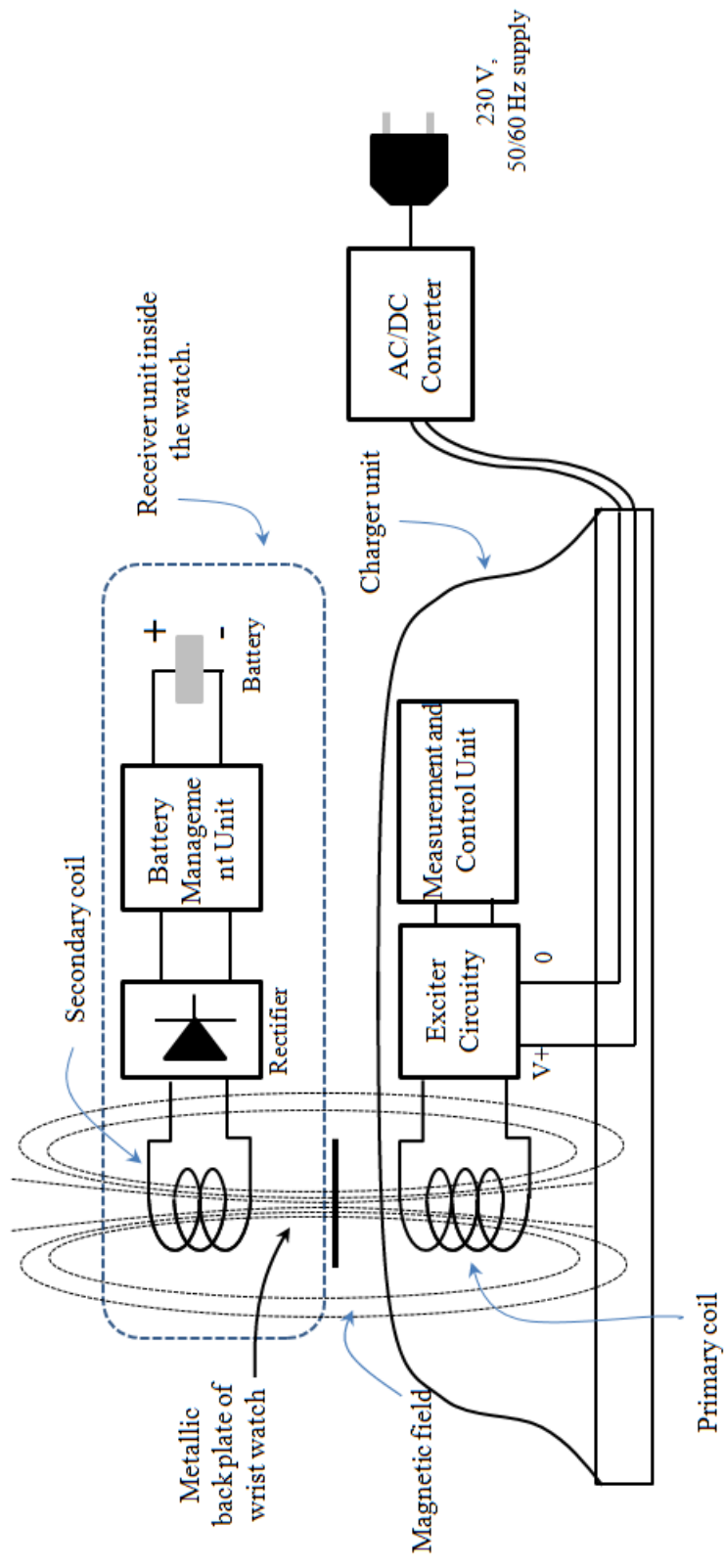


Figure 2.2: Basic schematic diagram of the IPT system. The receiver coil, rectifier and the associated electronic circuitry are to be kept inside the wrist watch.

2.2 Magnetic Circuit Design

A simplified drawing of the magnetic circuit of the primary (in the charging unit) and secondary parts (in the receiver unit) are shown in Fig.2.3. The 'U' shaped cores were used for both primary and secondary coil restrict the magnetic flux within the closed loop. A top view of the receiver part of the watch is given in Fig 2.4. Other than the core and coil, it also shows placement of some electronic components and ICs in a PCB required for conditioning the induced voltage to charge the battery.

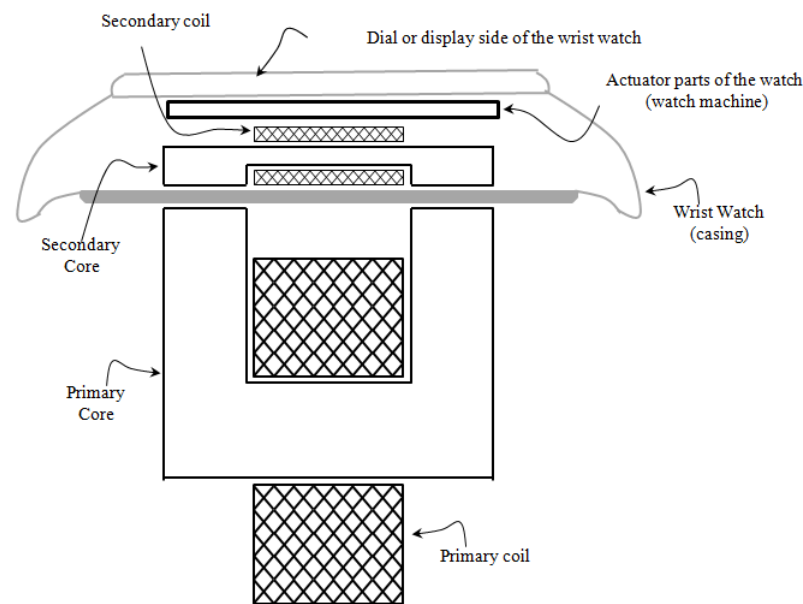


Figure 2.3: Magnetic Circuit (Side View).

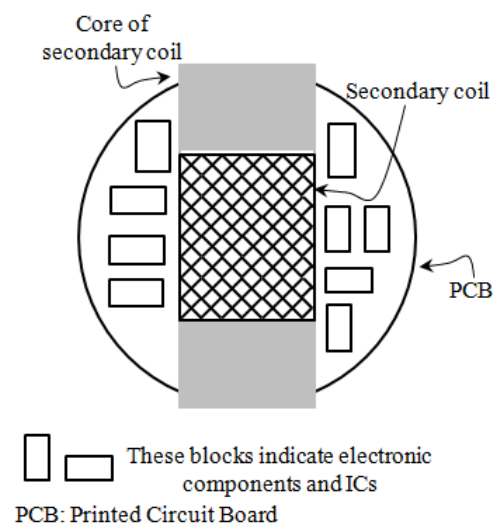


Figure 2.4: Top View of the receiver.

The magnetic circuit was first simulated using COMSOL. The flux density in the core is plotted in fig 2.5 and was found to be high near the areas where the coil is wound and low in the core limbs. Due to the presence of a large air gap (2.5mm on either limbs), the coupling between the two coils is low. Only a small portion of the flux generated by the primary coil links the secondary coil. Hence for a given flux density in the receiver core, the flux density in the transmitter core where the primary coil is wound is high. Due to this, there is a possibility that the core may get saturated and to avoid that PERMALLOY with a high saturation flux density value of 1.6 T is used. The effective permeability of the magnetic core is also very low.

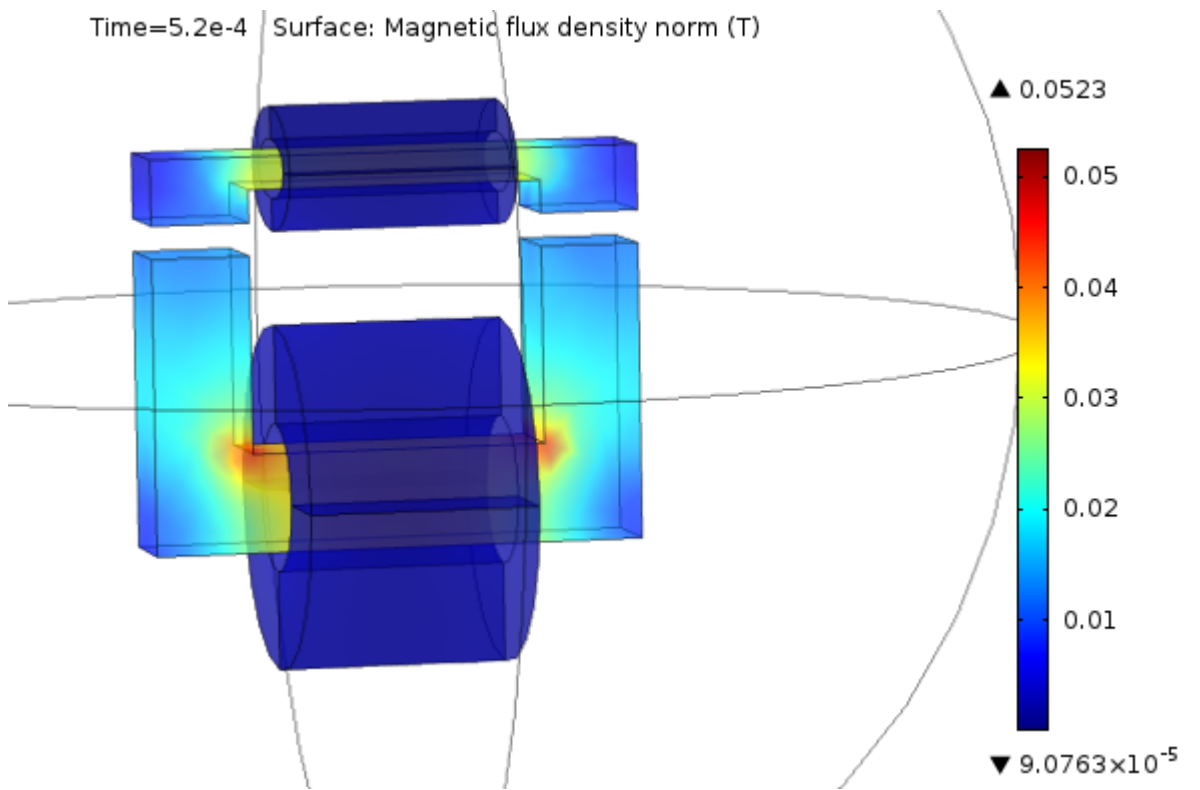


Figure 2.5: Flux density in the core.

2.2.1 Transmitter core

The transmitter coil is first wound over a bobbin. To make the 'U' shaped core, 'L' and 'I' shaped PERMALLOY pieces of thickness 0.5 mm are stacked as shown in Fig 2.6. The 'L' shaped piece goes through the bobbin and the 'I' shaped piece is kept at the other end to complete the 'U' shape. This is done to make the manufacturing process easier. The laminations should be insulated by a layer of varnish to reduce eddy current loss in the core. The dimension of the 'L' and 'I' pieces are also shown in Fig2.6. The

transmitter core dimensions are shown in Fig2.7. The bobbin dimensions are shown in Fig 2.8.

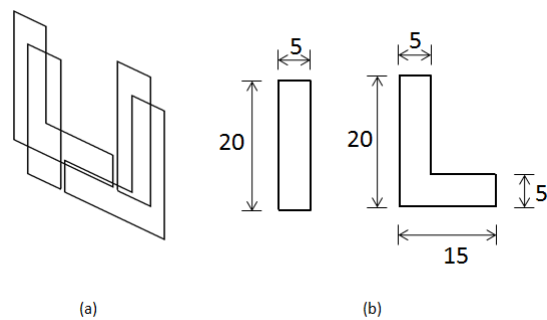


Figure 2.6: (a) shows the 'L' and 'I' pieces forming the 'U' shaped core. (b) shows the individual piece dimensions. All dimensions in mm

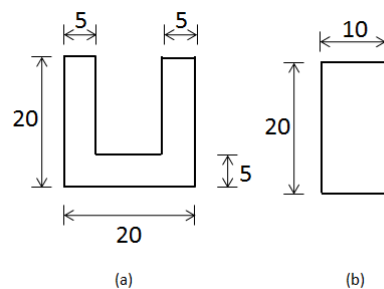


Figure 2.7: Transmitter core dimensions. (a) Front view and (b) Side view. All dimensions in mm

2.2.2 Receiver Core

The receiver core is made up by stacking a pair of small 'I' shaped PERMALLOY at either end of a larger 'I' shaped piece of the same material as shown in Fig 2.9. The pieces are held together by applying super glue at the edges. The coil is wound at the centre of the core in the space between the small 'I' pieces. The receiver coil dimensions are shown in Fig 2.10

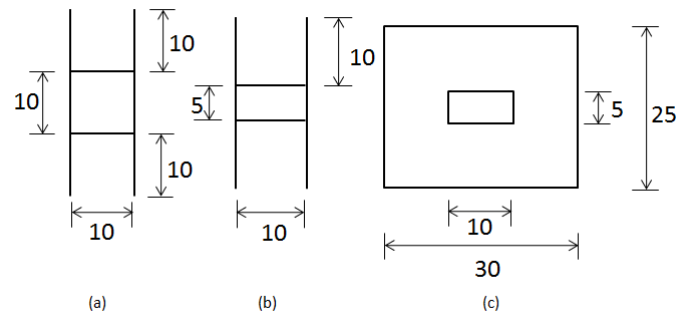


Figure 2.8: Bobbin Dimensions. (a) Front view, (b) Side view and (c) Top view. All dimensions in mm

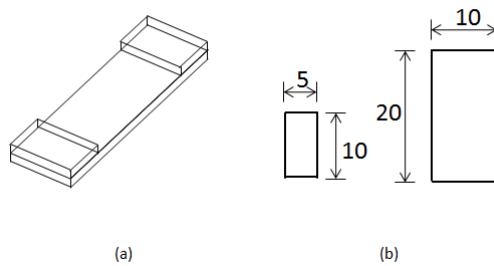


Figure 2.9: (a) shows the 'I' shaped pieces forming the 'U' shaped core. (b) shows the individual piece dimensions. All dimensions in mm

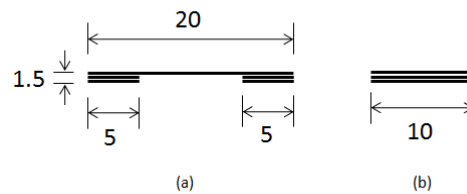


Figure 2.10: Receiver core dimensions. (a) Front view and (b) Side view. All dimensions in mm

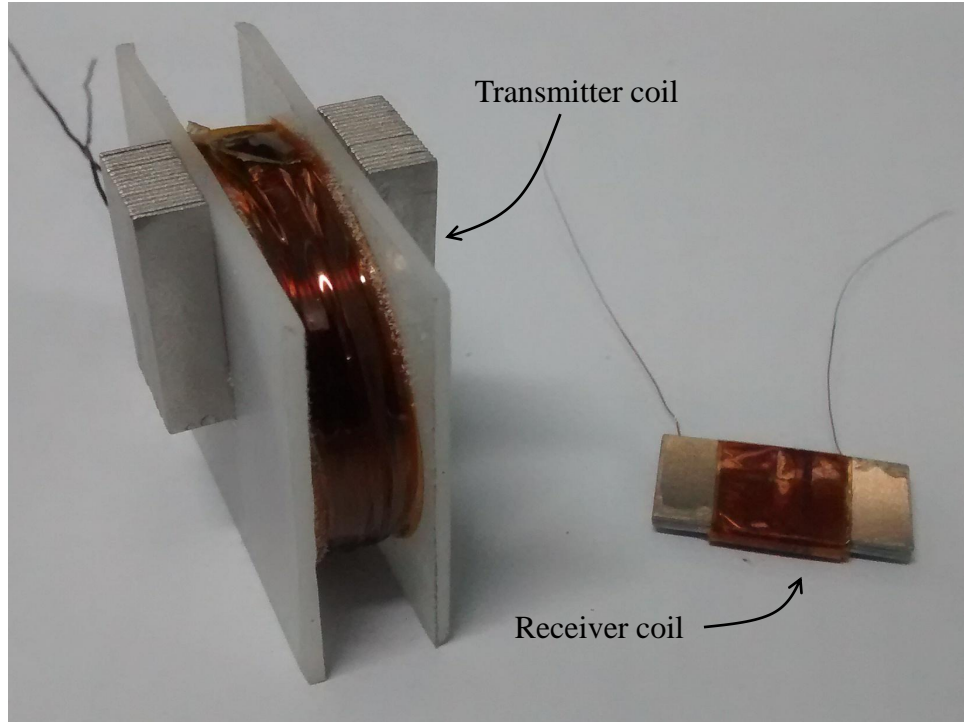


Figure 2.11: Transmitter and receiver coils developed

2.2.3 Coil Parameters

The coil parameters are given in Table 2.1. The inductance values are measured with the receiver coil kept on top of the transmitter coil with an air gap of 2.5 mm between them. The second coil is kept open when the inductance was measured.

Table 2.1: Transmitter and Receiver coil parameters.

<i>Parameter</i>	<i>Transmitter</i>	<i>Receiver</i>
No of turns	300	200
Wire gauge (SWG)	27	38
Inductance (mH)	12.1	1.5
Resistance (Ohm)	2.512	7.86

2.3 Transmitter Circuit Design

A simplified schematic diagram of the transmitter and receiver circuit is given in Fig 2.12. The primary coil L_p is excited from a DC source voltage using switches S_1 to S_4 which is connected in a H-bridge configuration. The control signals for these switches, ϕ_1 and ϕ_2 are generated by the MCU. A capacitor C_p is connected in series with L_p and

together they form a series resonant circuit at a frequency f_{CH} . This enables to pass maximum current (for a given source with finite internal impedance) through L_p and voltage across L_p will be maximum at this frequency. As this forms a band-pass filter (with centre frequency f_{CH}), the current through L_p and hence the magnetic field produced is sinusoidal in nature, rather than a square wave (that increases the iron losses). C_p also improves the power factor of the load as seen from the exciter circuit.

Switch S_6 and S_7 are used to switch the excitation voltage between V_{CH} and V_D . V_{CH} is used when charger is charging the watch battery and V_D is used when it is searching for the watch. Each switch S_1 to S_4 has a freewheeling diode connected in parallel for protection against voltage spikes across L_p during switching. Two zener diodes are connected back to back parallel to L_p to limit the voltage across it. The voltage v_c at the node between L_p and C_p is given to the non-inverting terminal of a comparator IC and its output along with the switching pulse ϕ_2 is given to the AND gate. The output from the AND gate is given to the MCU. The width of this pulse is used for watch detection, watch removal detection etc. which will be explained in the next chapter. The negative supply required for the comparator IC is generated using a charge pump voltage inverter IC. The complete transmitter circuit diagram is given in Fig 2.13.

2.4 Receiver Circuit Design

The voltage induced in the receiver part coil L_s is available across a capacitor C_s . Another capacitor C_{s1} and a switch S_5 can also be seen in the circuit. The voltage across C_s is bipolar, which is converted to a uni-polar voltage with the help of a bridge rectifier unit using the four Schottky diodes. The voltage drop across each diode is only 100mV. This full-wave rectified voltage is then available across the capacitor C_{FL} , which helps to reduce the ripples as in a standard rectifier unit.

The rectified voltage is fed to a battery management IC, which controls the charging process of the battery. Once the battery is fully charged, management IC will give an indication by setting its STAT pin to high. This will close the switch S_5 , which will bring capacitor C_{s1} in parallel with C_s . This will change the resonant frequency (which can be detected from the charging unit) and is used as an indication of completion of

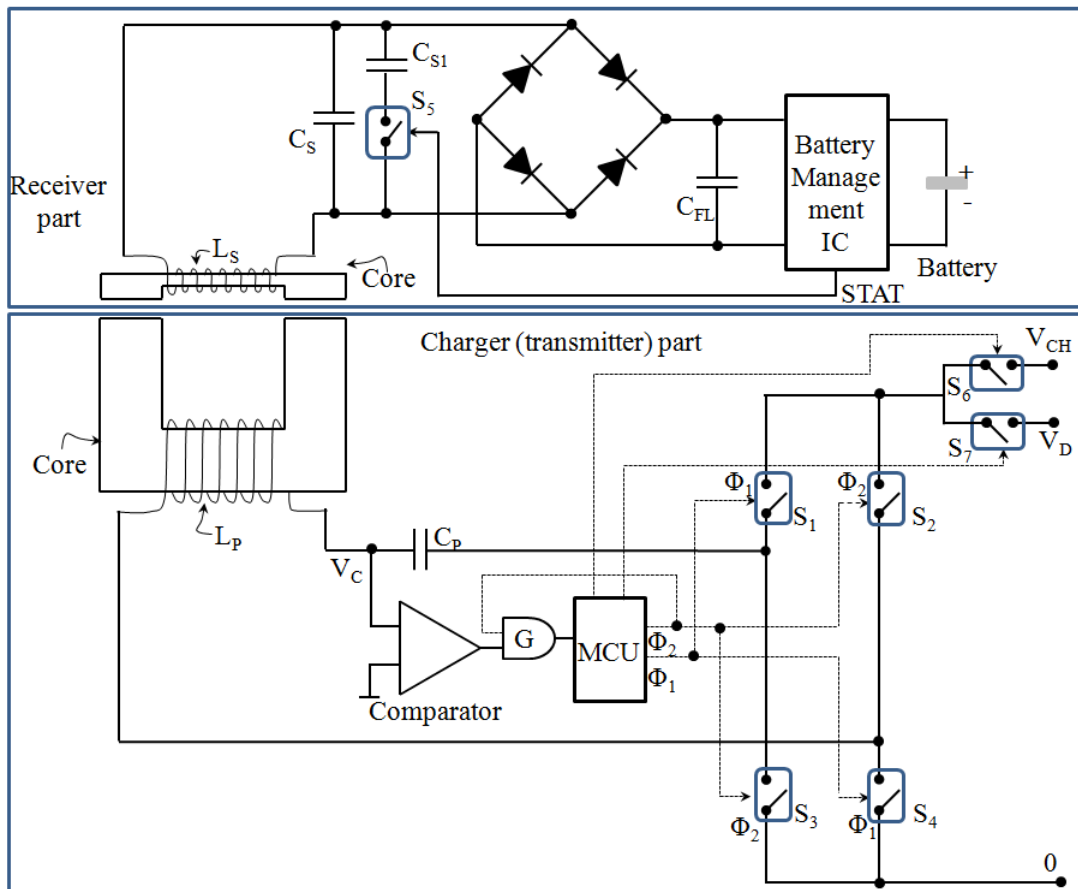


Figure 2.12: Transmitter and receiver circuit schematic diagram.

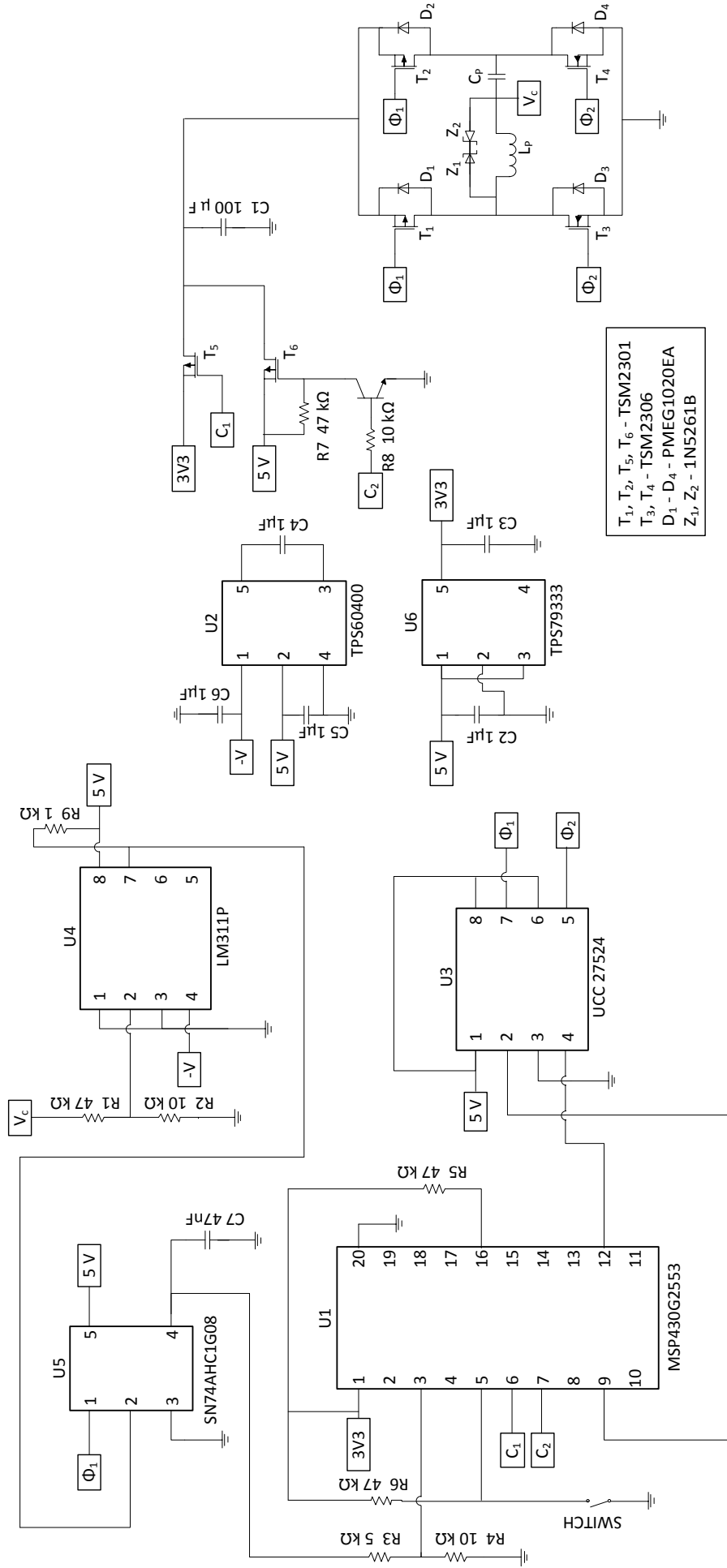


Figure 2.13: Complete Transmitter circuit.

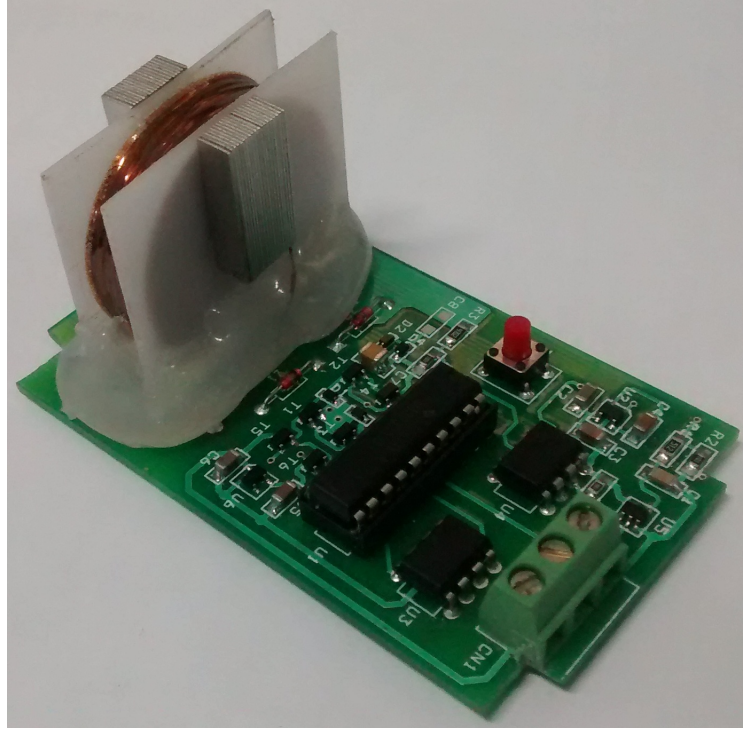


Figure 2.14: Transmitter circuit fabricated on PCB. The transmitter coil, the MOSFET H-bridge, driver IC, MCU and the signal conditioning circuits can be seen.

the charging process. This feature is available only for watches with 3.6 V battery as battery management IC is available only for this voltage level. The 33 k Ω resistor is connected to the IC to set the maximum charging current as 30 mA.

For watches with 3 V, 2.3 V and 1.5 V batteries a timer based solution is provided where the charger will automatically stop charging after 5 hours. These batteries usually take a long time to get fully charged 1.6 but in 5 hours they can be charged to a reasonable level from a fully discharged state. The rectified output is fed to a voltage regulator IC and then connected to the battery through a diode and a current limiting resistor. A diode with a very low leakage current is selected to prevent the battery from getting drained through the diode. The complete receiver circuit diagram is given in Fig 2.15 and 2.16.

2.5 Selection of Charging Frequency

IPT systems designed to transmit power through non conductive medium are operated at high frequencies in the range of 100 kHz and above. At these frequencies the mag-

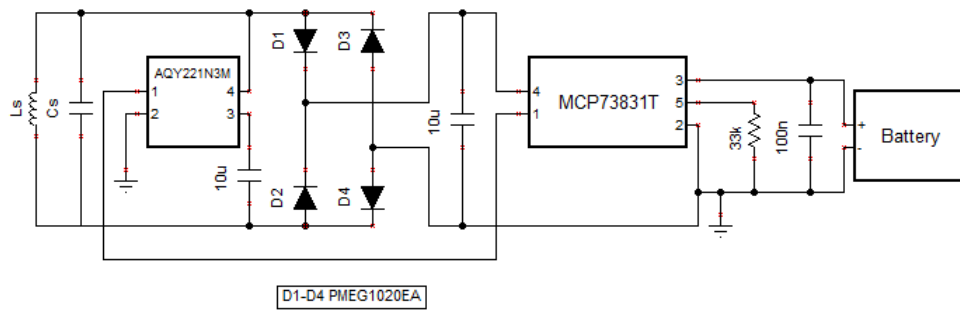


Figure 2.15: Receiver circuit for 3.6 V battery.

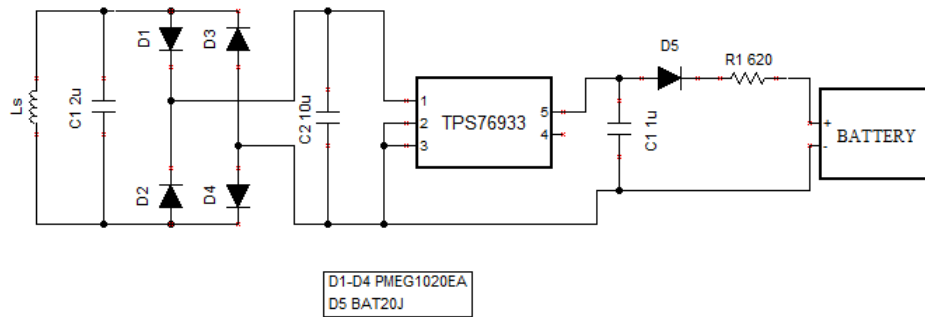


Figure 2.16: Receiver circuit for 3 V battery. This can also be used to charge 2.3 V and 1.5 V battery by changing the voltage regulator IC and the series resistor

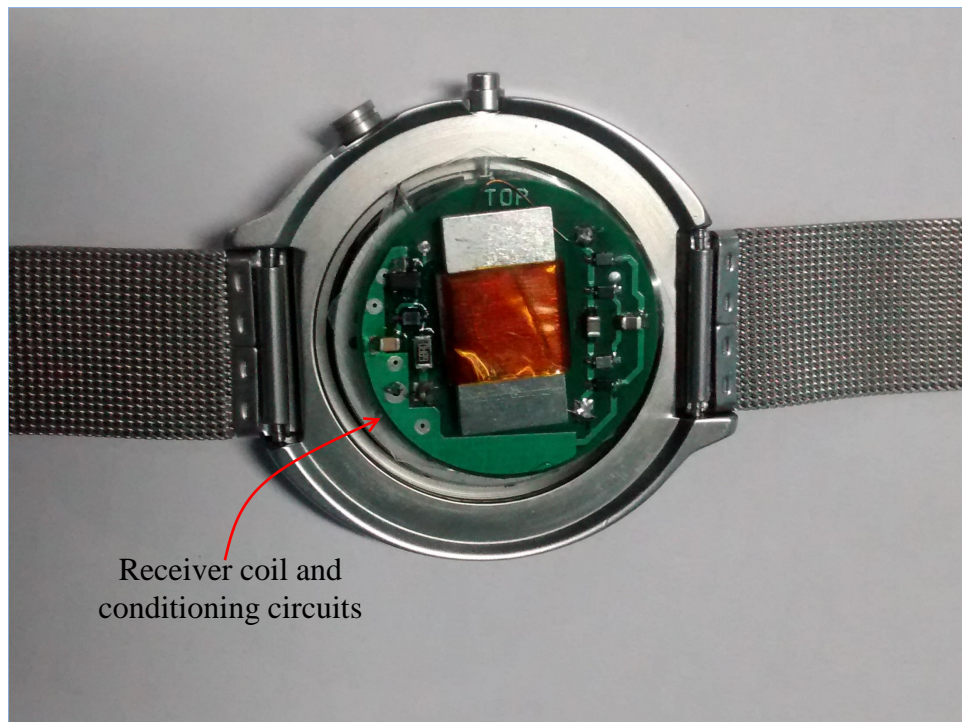


Figure 2.17: Receiver circuit fabricated on PCB and fixed inside the watch. Picture taken without back plate to show the receiver part

netic field required to transfer a given amount of power is low which means the current through the coil is low and hence copper losses would be minimum. But when power has to be transferred through a conductive medium we have to take into account its skin effect also. The skin depth for a particular frequency is given by the (2.1) where σ is the conductivity of the metal, μ_0 the permeability of free space and μ_r its relative permeability.

$$\delta = \frac{1}{\sqrt{\pi f \sigma \mu_0 \mu_r}} \quad (2.1)$$

The watch back plate is made of stainless steel which can have a maximum μ_r value of 7 and conductivity $\sigma = 1.45 \times 10^6 \Omega\text{-m}$. At $f = 6000 \text{ Hz}$, which is the watch detection frequency (f_D), skin depth $\delta = 2 \text{ mm}$. The thickness of the watch back plate currently used is 1.25 mm. The frequency chosen leaves enough margin to account for the variability of these parameters. The watch is charged at 4200 Hz.

CHAPTER 3

CHARGER FEATURES AND ITS IMPLEMENTATION

3.1 Introduction

The IPT charger is designed to have the following features each of which is explained in the sections below.

- Watch Detection
- Watch Removal Detection
- Charge Complete Detection
- Battery type Detection

3.2 Watch Detection

The IPT charger system should be able to detect the IPT enabled watch when it is kept on the charger and only then it should start charging. This ensures that the magnetic field around the charger is minimum when it is not charging. It also helps to bring down the no load losses as the primary coil is not excited when charger is in idle state.

In the receiver circuit a capacitor C_s is kept parallel to L_s and this has a resonance frequency f_D . The bode plot of v_c with and without C_s connected across L_s is shown in Fig 3.1. There is a resonant peak in the phase plot at the frequency f_D . Only a parallel resonant circuit with resonance frequency close to f_D can produce such a peak at that frequency in the phase plot. To measure this phase angle the voltage v_c is given to the non-inverting terminal of a comparator IC and its output along with the switching pulse ϕ_2 is given to the AND gate. The output from the AND gate, v_g is given to the MCU. The on time of this pulse v_g was found to be proportional to the phase angle and is

measured by the MCU. The bode plot is generated using LTSPICE, a SPICE simulator from Linear Technology.

The waveforms ϕ_1, ϕ_2, v_c and v_g with and without C_s is shown in Fig 3.2. The pulse width of v_g is higher when C_s is present. If this width is within the threshold value, the object kept on the charger is identified as a watch. The IPT charger was further tested by placing coins, key chains etc. on top of it and only a receiver with resonant frequency f_D was detected as a watch.

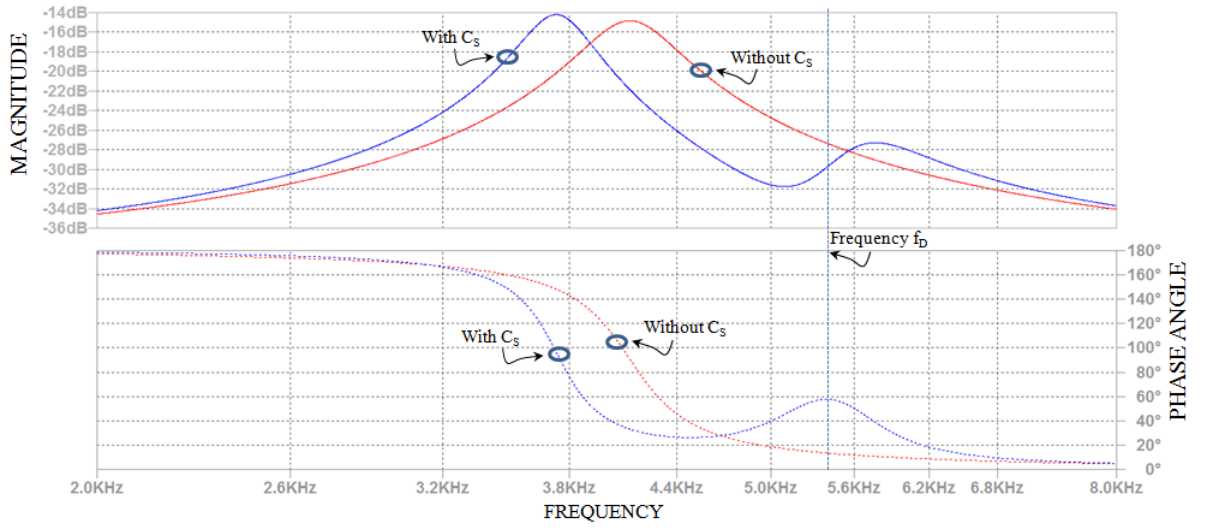


Figure 3.1: Bode plot of v_c with and without C_s . The phase angle at f_D is measured for watch detection

3.3 Watch Removal Detection

The charger should stop charging once the watch is removed from the charger. When the watch is kept on the charger, the magnetic flux is restricted to the magnetic core and once the watch is removed from it, a low reluctance closed path is no longer available for the magnetic flux. The charger should now stop charging to reduce the field around the charger.

The inductance of the primary coil will match the designed value only when the receiver core is kept on top of it. When the receiver coil is removed, the magnetic path provided by the core is now open and its reluctance increases, reducing the primary coil inductance. This changes the resonant frequency at the transmitter side and the

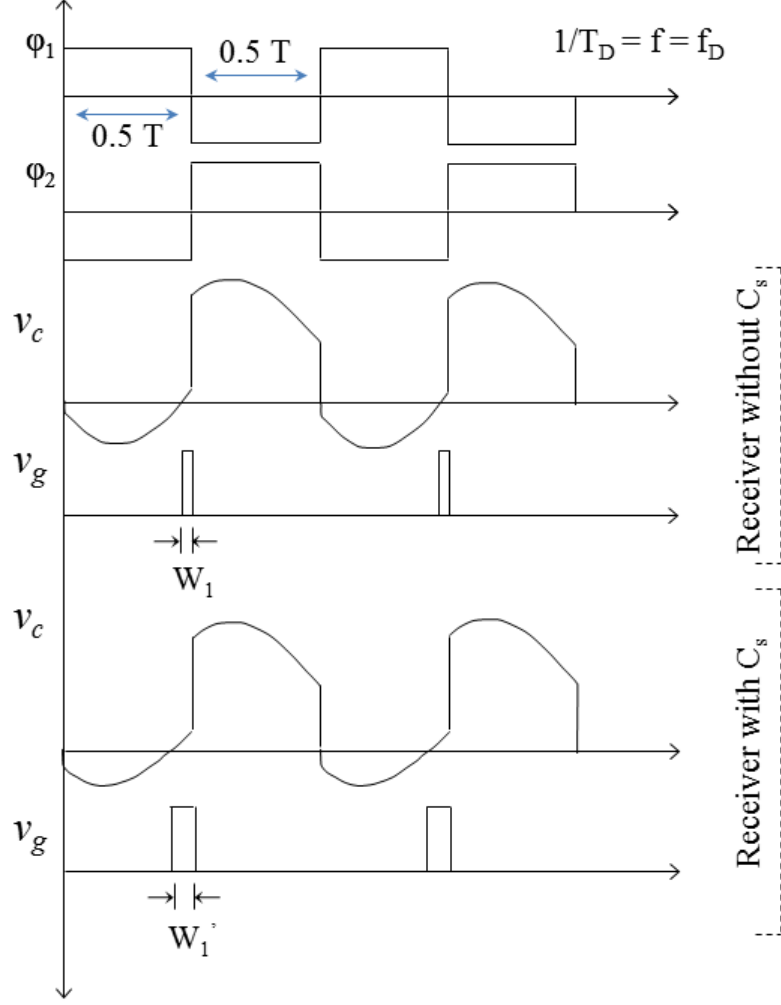


Figure 3.2: ϕ_1, ϕ_2, v_c and v_g with and without C_s

phase plot shifts to the right as shown in Fig 3.3. The phase angle at the frequency f_{CH} increases, the pulse width of v_g measured by the MCU exceeds the threshold and the charger stops charging. The waveforms ϕ_1, ϕ_2, v_c and v_g with and without watch kept on charger is shown in Fig 3.4.

The phase measured by MCU under different conditions is plotted in Fig 3.5. It matches with the simulated results.

3.4 Charge Complete Detection

Once the charging is complete the charger should stop charging. This reduces the no load power consumption of the charger, making the system more energy efficient.

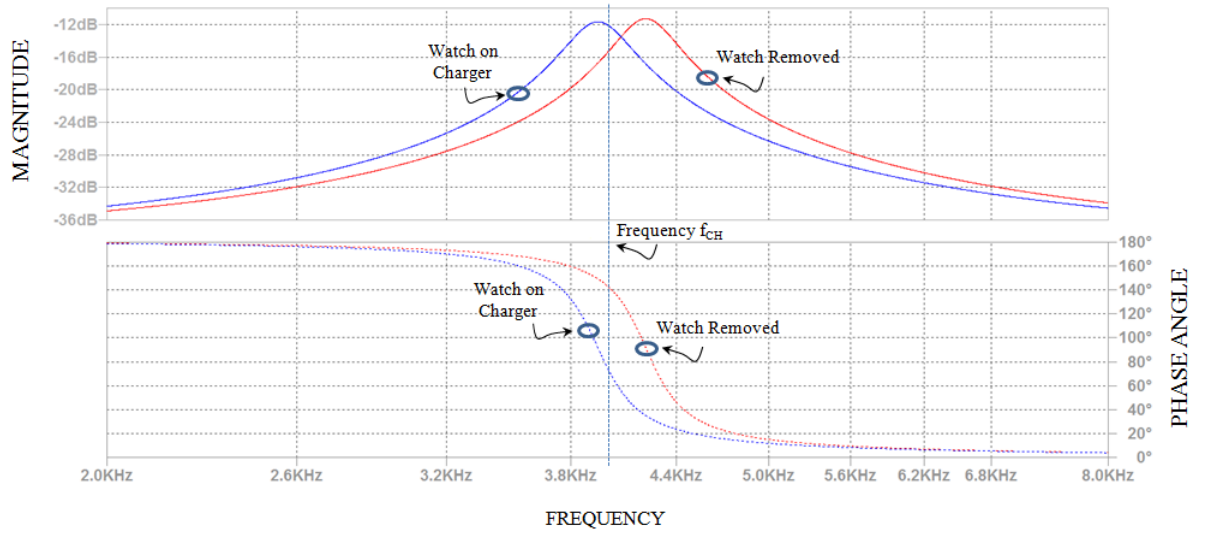


Figure 3.3: Bode plot of v_c with and without the watch on the charger. The phase angle at f_{CH} is measured for watch removal detection

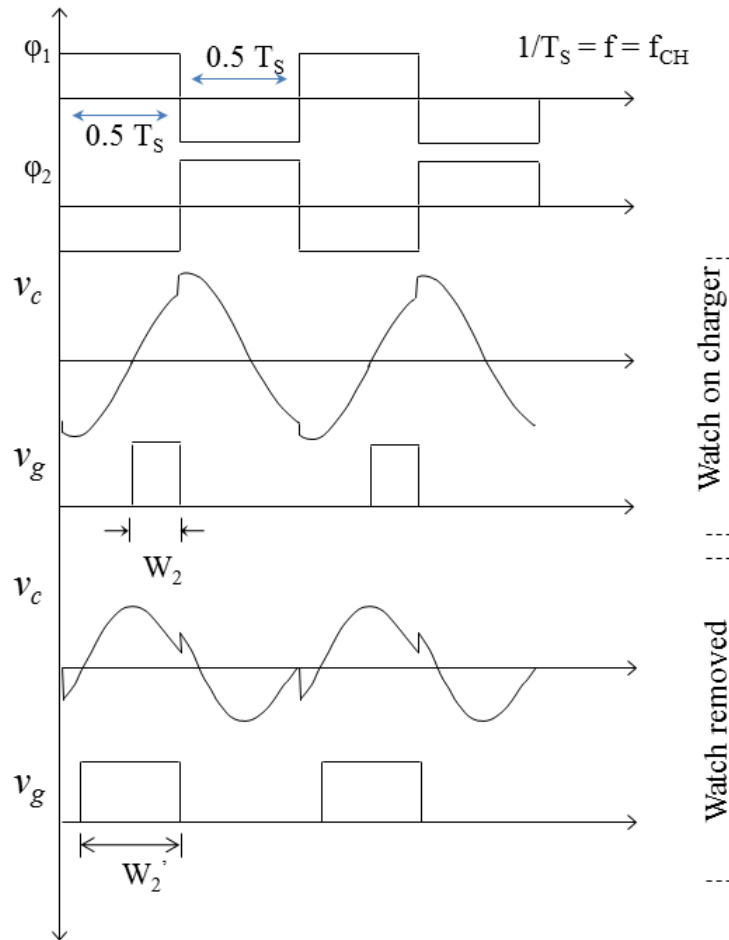


Figure 3.4: ϕ_1 , ϕ_2 , v_c and v_g with and without the watch on the charger.

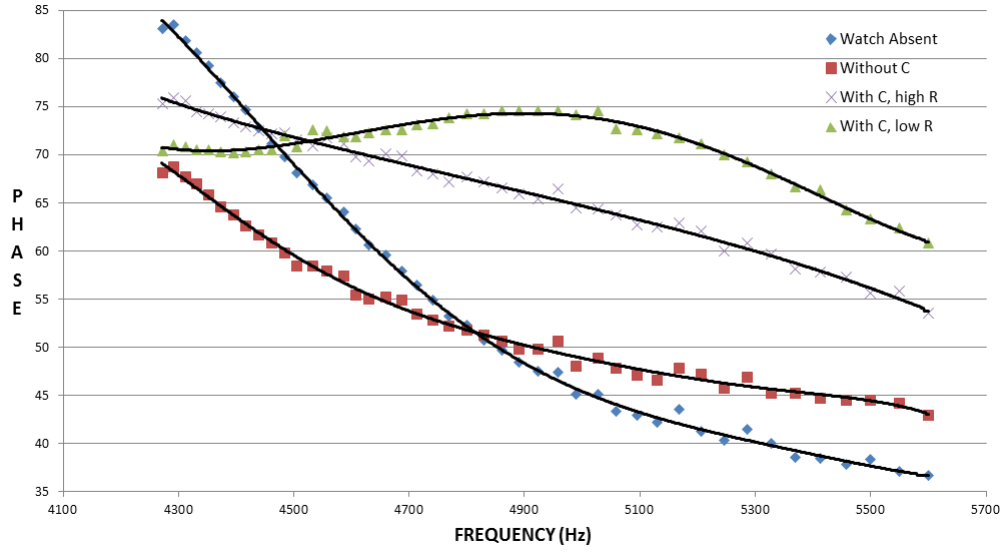


Figure 3.5: Phase measured by MCU

When the battery is fully charged the STAT pin of the battery management IC becomes high. This will close the switch S_5 bringing the capacitor C_{s1} in parallel to C_s . This makes the secondary resonance frequency lower than f_{CH} and the bode plot is now as shown in Fig 3.6. At f_{CH} the phase measured will now be higher and if it is greater than the threshold set, the charging is stopped. This feature is currently available only for watches with 3.6 V battery. For lower voltage batteries, charging is automatically stopped after 5 hours.

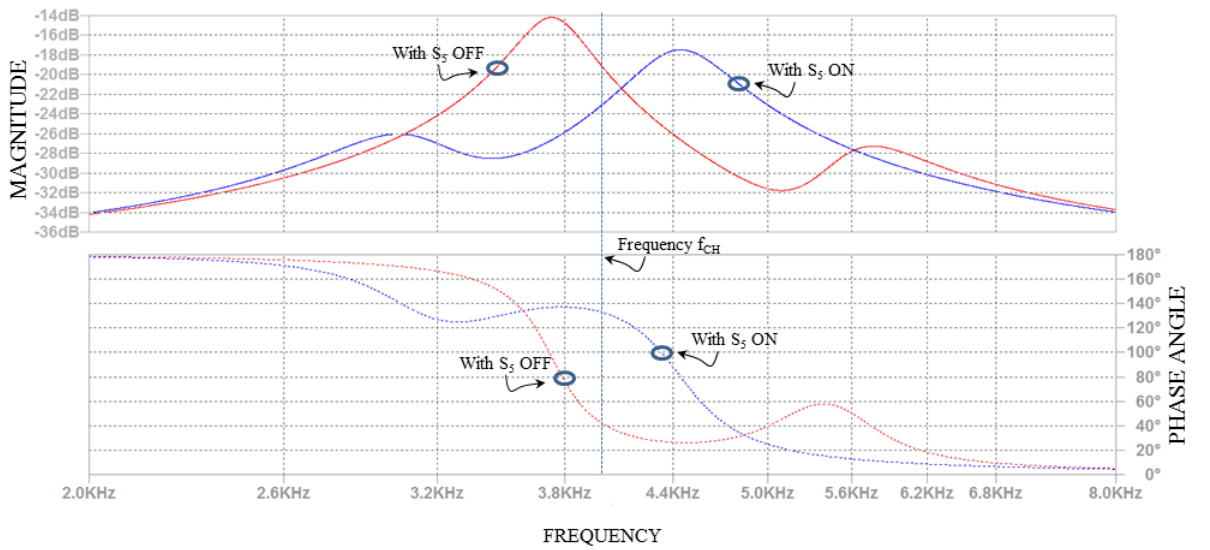


Figure 3.6: Bode plot of v_c with S_5 on and off. The phase angle at f_{CH} is measured for charging complete detection

3.5 Battery Type Detection

The rechargeable batteries used in the watches can be classified into two types.

- Low capacity batteries typically in the range of 10 mA-h with a maximum charging current of 2 mA.
- High capacity batteries in the range of 120 mA-h or above. The 120 mA-h battery permits a maximum charging current of 80 mA.

For low capacity batteries, since the charging current is low the total impedance seen from the input side is low and hence the current flowing through the primary coil is high. This in turn increases the magnetic field produced by the coil which increases the eddy current losses in the metallic back plate causing its temperature to rise beyond the allowed limit. To prevent this the charging current has to be reduced. This can be achieved by increasing the charging frequency. The impedance seen from the input side is now high, thereby reducing the current through the primary coil. For high capacity batteries, the charging current is high and hence the impedance seen from input side is high allowing it to be charged at a frequency close to the primary resonance frequency.

Therefore to prevent the overheating of the watch back plate it is very important to detect the type of battery in the watch. The secondary resonance frequency for the receiver circuit of watches with low power battery is set at a much higher value. When the pulse width of v_g is measured at that frequency, only these watches give a value which is above the threshold and thus they can be detected by the charger. Thus the same charger can be used for all the watches.

3.6 Charging Algorithm

The flowchart of the charging algorithm is given in Fig 3.7. During the search mode a reduced voltage V_D is applied to the primary coil to limit the magnetic field around the charger. When the IPT enabled watch is kept on the charger, width of the pulse v_g is greater than the threshold set and the charger goes into charging mode. If after 'b' iterations a watch is not detected the charger goes into standby mode. A reset switch is provided to wakeup the charger to start searching for watch again.

In the charging mode the excitation voltage is changed to V_{CH} . When the IPT enabled watch is kept on the charger, the magnetic path is complete. Most of the magnetic field is now through the core and that around the charger will be low. The width of v_g is measured after each 5 seconds. The width exceeds the threshold when either the watch is removed from the charger or when the battery is fully charged and the charger then goes back to search mode. If the watch has been removed the charger continues in search mode finally goes into standby mode. But when the battery is fully charged the charger still detects the watch during search mode and it goes into charging mode. This is because during search mode the receiver coil output which is given to the battery management IC is not high enough and the STAT pin output will be zero. This opens the switch S_5 and the resonant peak in the bode plot is now back. The width of v_g measured will be high and the charger goes into charging mode. Once in the charging mode the STAT pin becomes high sending the charger back to the search mode. If this process repeats for 3 times the charger assumes that the battery is fully charged and stops charging.

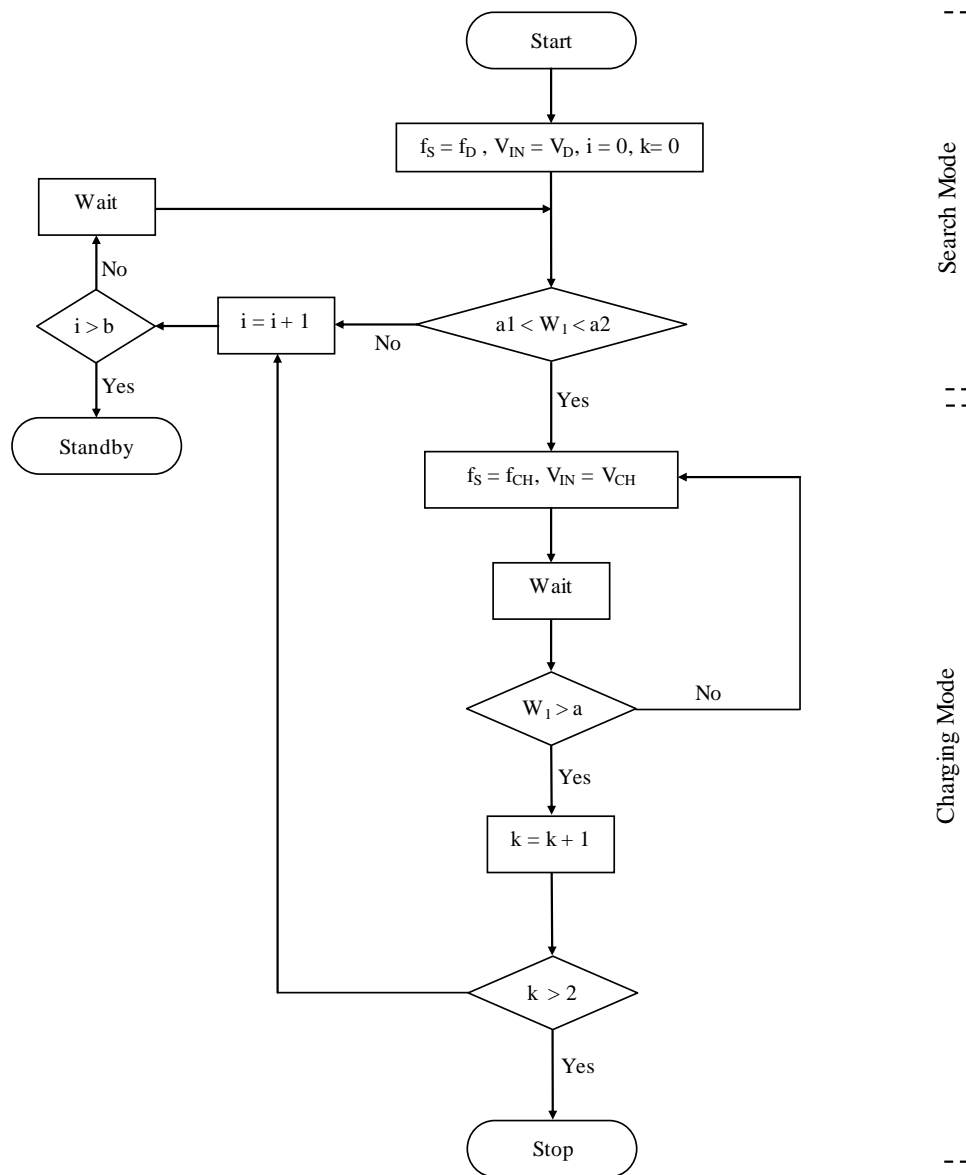


Figure 3.7: Charging algorithm flowchart

CHAPTER 4

RESULTS AND EVALUATION

4.1 Results

The transmitter and receiver circuits were fabricated on a PCB and tested. The voltage waveforms v_g and v_c were found to be consistent with the simulation results. These waveforms under the different conditions were observed on the Tektronix MSO 2014 Mixed Signal Oscilloscope and are shown below.

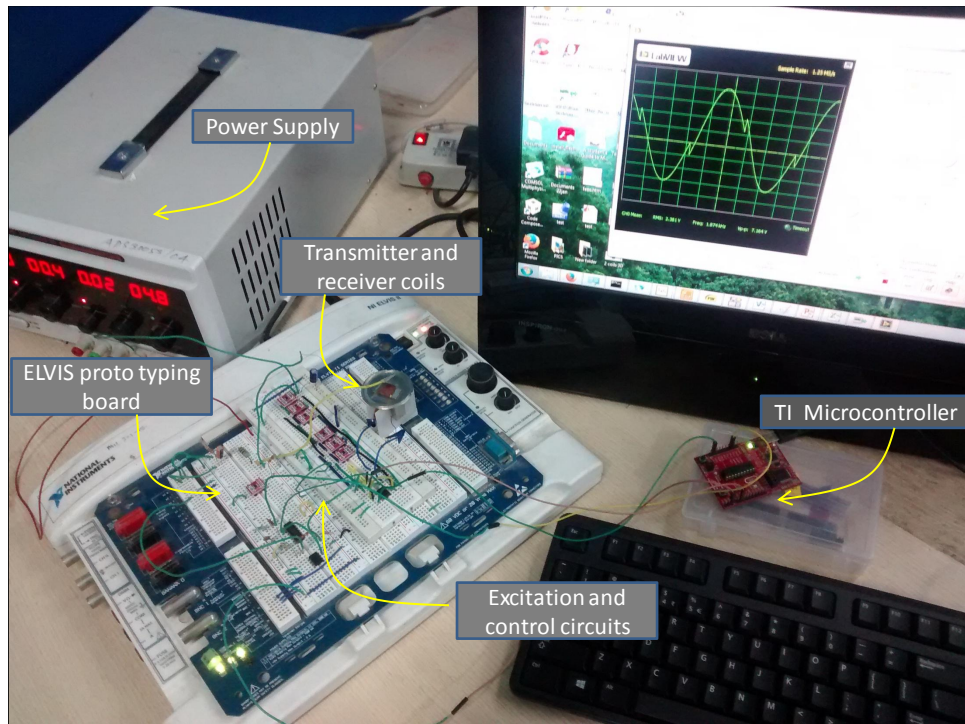


Figure 4.1: Test setup showing the prototyping board, power supply, micro controller and the excitation and control circuits

The transmitter circuit assembled on a PCB is kept inside a plastic box over which the watch can be placed as shown in Fig 4.9 for charging. A receiver coil with its output connected to an LED is placed on top of a charger and the glowing LED indicated that the receiver is getting power from the charger, Fig 4.10.

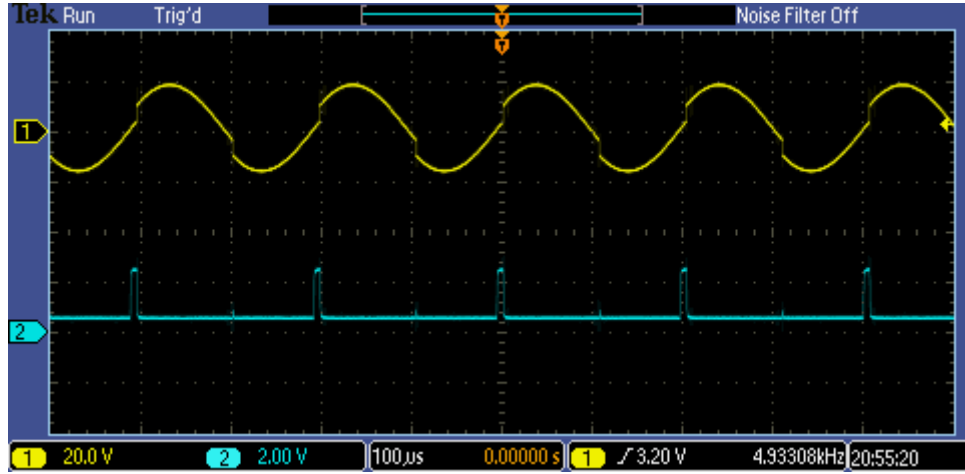


Figure 4.2: v_c and v_g during search mode when C_s is not connected across the receiver coil L_s . The same waveform is observed when a coin is kept on the charger.

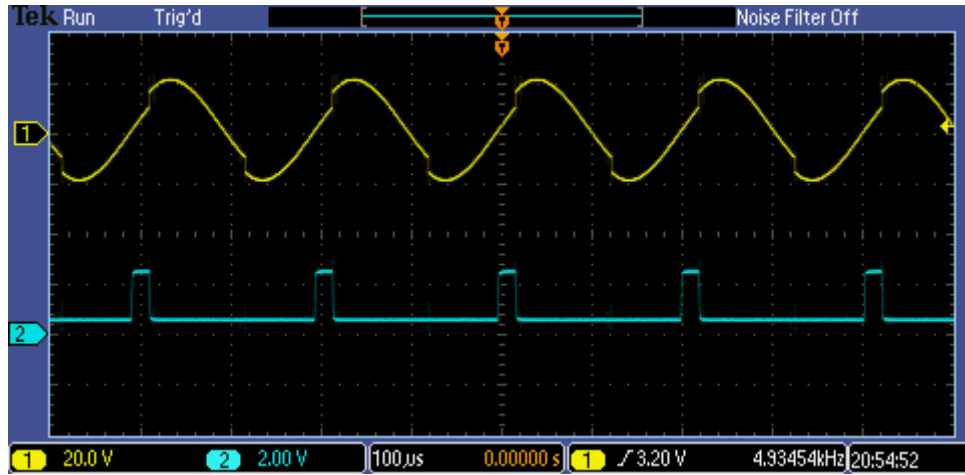


Figure 4.3: v_c and v_g during search mode when an IPT enabled watch is kept on charger. Width of v_g increased when watch was kept on charger

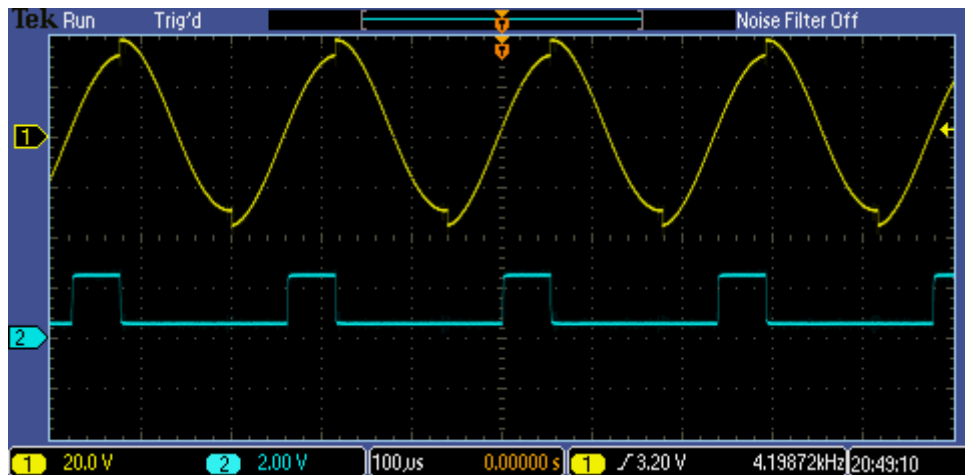


Figure 4.4: v_c and v_g during charging mode when an IPT enabled watch is kept on the charger. The width of v_g is greater when the charger is in charging mode.

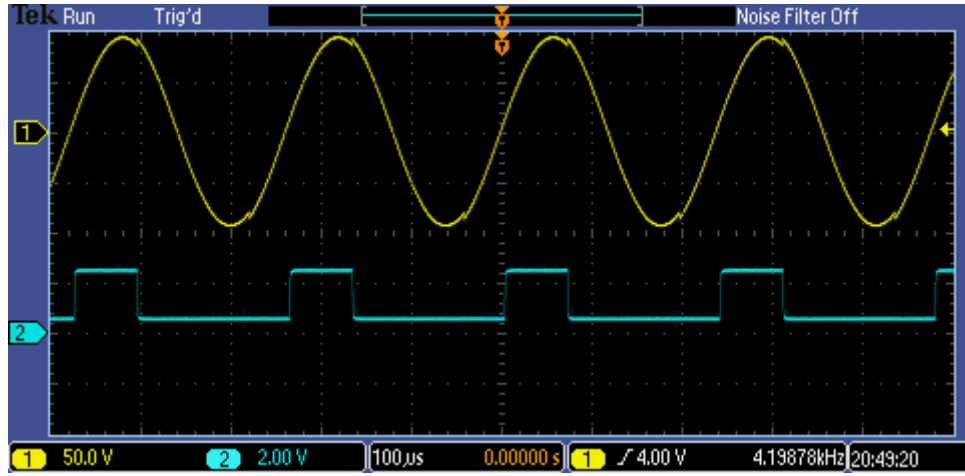


Figure 4.5: v_c and v_g during charging mode when the watch is removed from the charger. The pulse width of v_g has now increased. The magnitude of v_c has also increased as effective impedance seen from input side reduced.

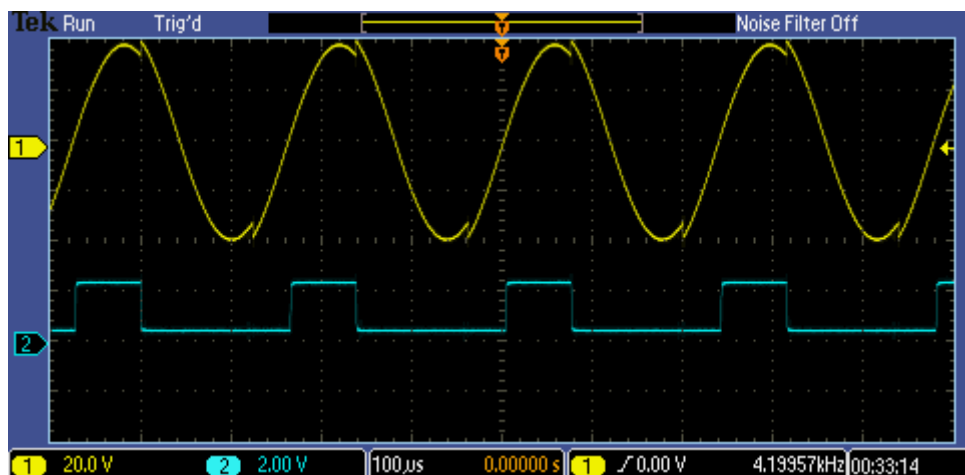


Figure 4.6: v_c and v_g during charging mode when watch battery is fully charged. The pulse width of v_g is greater than when in charging mode.

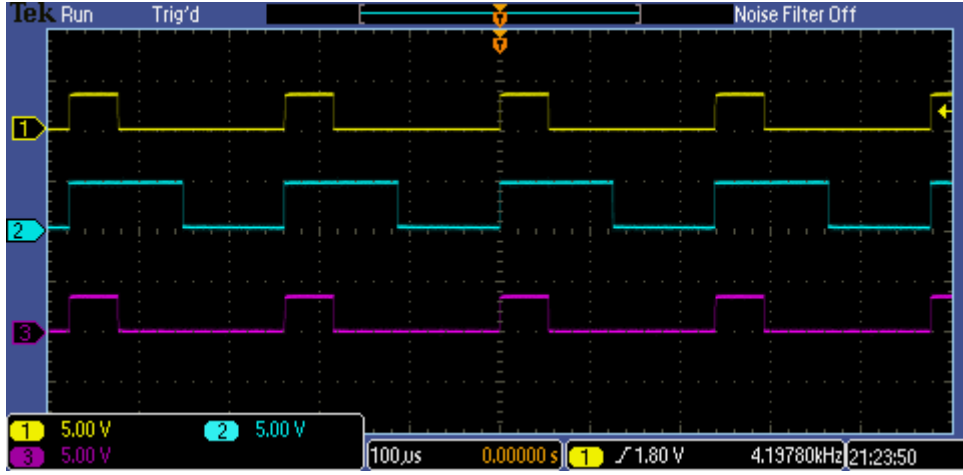


Figure 4.7: The comparator output, and the switching pulse ϕ_2 which are given as input to the AND gate and its output v_g plotted in that order when the watch is being charged

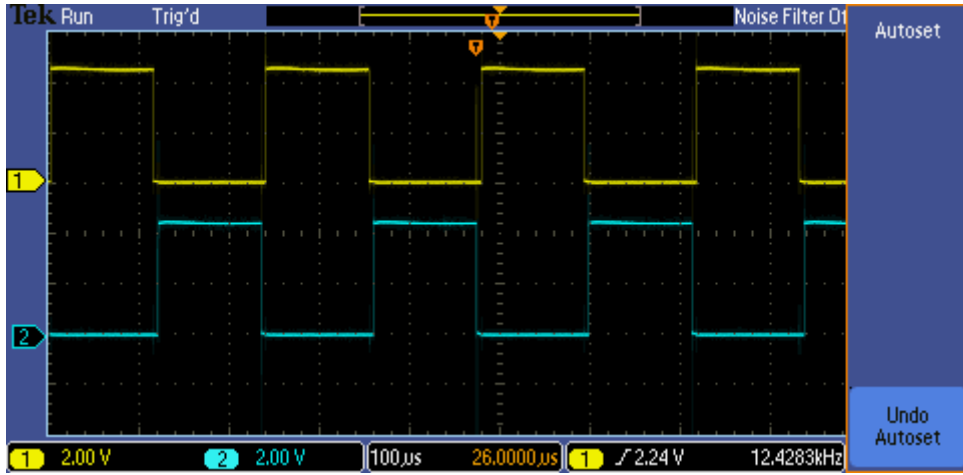


Figure 4.8: The non overlapping switching pulses ϕ_1 and ϕ_2 generated by the MCU. They drive the MOSFET H-bridge which powers the primary coil.

4.2 Efficiency Analysis

The major factors contributing to losses in the charger are copper losses in the windings and the core losses. The power transmitted to the battery is low and hence these losses become significant. The core loss is determined by no load test on the transformer. To separate the core losses no load test is done at two different frequencies keeping current through L_p same. The copper loss in the primary can be calculated from coil current. These losses plus the output power is subtracted from the input power to the coil to get the secondary coil losses (which is difficult to measure directly) and the loss in the rectification stage inside the watch.

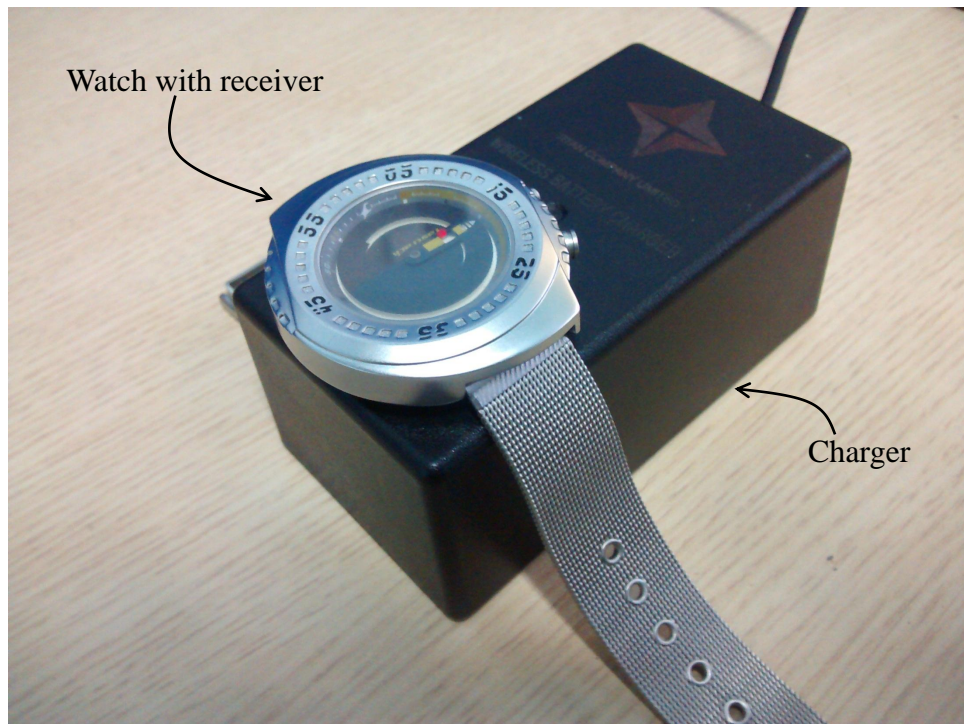


Figure 4.9: The IPT enabled watch kept on the charger developed.

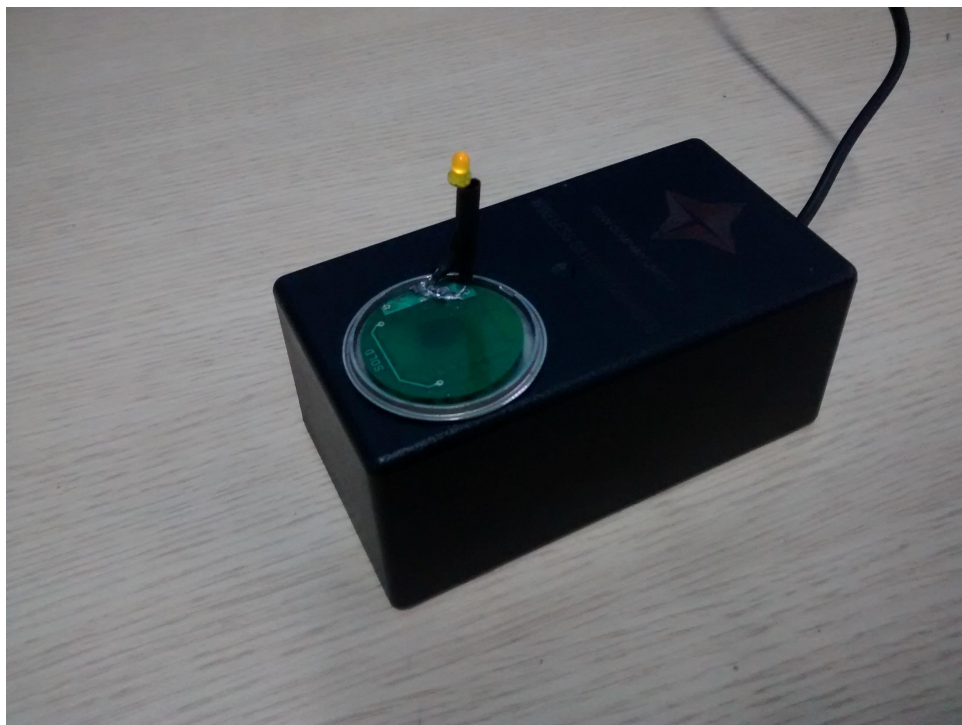


Figure 4.10: Receiver circuit with an LED connected at its output to show its operation receiving power from the charger

4.2.1 Core loss measurement

The core loss is measured by no load test. When a transformer is operated at no load conditions, the current through the primary is low and hence core loss can be neglected. The power measured across the coil is mainly the core losses. For a loosely coupled transformer the no load current is high (due to low effective permeability of the magnetic path) and so the copper losses cannot be neglected. The current through the coil is kept the same as that during the loaded condition so that the core loss will be same in both the cases. The coil is excited at the charging frequency $f_{CH} = 4200$ Hz. The readings taken are given below.

Voltage across coil (V_{L_p})	23.19 V
Current through coil (I_{L_p})	121.3 mA
Power measured across coil (P_{coil})	142 mW
Power Factor	0.05
Primary winding resistance R_{L_p}	2.512 Ω
Copper loss P_{copper}	36.8 mW
Core loss P_{core}	105.2 mW

4.2.2 Separation of core loss

The core loss components include eddy current loss (P_e) and hysteresis loss (P_h). We have

$$\begin{aligned} P_e &\propto (B_m)^2 f^2 \\ P_h &\propto (B_m)^{1.6} f \end{aligned} \tag{4.1}$$

where B_m is the peak magnetic field in the core and f is the frequency. The experiment is done at two different frequencies keeping I_{L_p} and hence B_m same. The core loss can now be written as in (4.2) and this equation satisfies the P_{core} measured for the two frequencies. A is the proportionality constant for P_e and B that for P_h . The readings taken are given in table 4.1. Solving (4.2) for these two frequencies, we get P_e as 62.5 mW and P_h as 42.63 mW at $f = 4200$ Hz. To reduce P_e the core laminations has to be

insulated. This is yet to be done and once they are insulated P_e will come down.

$$P_{core} = Af^2 + Bf \quad (4.2)$$

Table 4.1: No load test for separation of core losses.

<i>Frequency</i> (Hz)	V_{L_p} (V)	I_{L_p} (mA)	P_{coil} (mW)	P_{copper} (mW)	P_{core} (mW)
3462	19.32	120.7	114	36.2	77.8
4200	23.19	121.3	142	36.8	105.2

4.2.3 Efficiency under loaded conditions

The efficiency of the charger was measured at $f_{CH} = 4200$ Hz keeping a load resistance R_L of 98Ω . The readings taken are given below. Since I_{L_p} is same, P_{core} will be same as that measured during no load test.

P_{in}	552 mW
V_{L_p}	22.33 V
I_{L_p}	121.1 mA
P_{coil}	398 mW
Power Factor	0.15
Load resistance R_{L_p}	98Ω
P_{out}	194 mW
Copper loss in primary coil	36.8 mW
Core loss P_{core}	105.2 mW
Power loss in receiver side	62 mW
Efficiency η	35.2 %

The efficiency of the charger was measured at different load conditions keeping the output induced voltage same (table 4.2) and as expected it reduced when the load was reduced. This charger works efficiently only while charging the 3.6 V battery where the charging current is high. When charging the low voltage battery, say the 1.5 V battery

the output power delivered is 6 mW which is lower than the power loss across the AC to DC converter used.

Table 4.2: Efficiency under different load conditions

<i>Load Resistance</i> (Ω)	<i>Load Current</i> (mA)	<i>Efficiency</i> (%)
100	45	35.2
220	20.4	22.9
440	10.2	14.26
2700	1.67	2.7

4.3 Coefficient of Coupling k

Due to the air gap in the magnetic circuit the coupling between the primary and secondary coil is very low. The coupling coefficient can be calculated by (4.3) where L_{sc} is the primary coil inductance measured with secondary coil shorted while L_p is the same measured with secondary open.

$$k = \sqrt{1 - \frac{L_{sc}}{L_p}} \quad (4.3)$$

The measured values of L_{sc} and L_p are 6.6 mH and 7.3 mH giving a coupling coefficient $k = 0.32$.

CHAPTER 5

CONCLUSION AND FUTURE WORK

5.1 Conclusion

An IPT based charger system was designed and fabricated for wrist watches. The conventional wireless chargers available cannot transmit power through metal surfaces as they operate at a high frequency. The system developed operate at a frequency much lower than the limit set by skin effect of the metallic back plate. The receiver circuit dimensions are within a diameter of 20 mm with a thickness of 2.3 mm and can easily fit inside the watch. Watch detection, watch removal detection etc. are all done from the charger itself, making the receiver circuit small. The charger can transmit power through the stainless steel back plate of the watch without heating it beyond the permissible limits.

Batteries of different voltage levels can be charged using the same charger. The charger can detect the presence of an IPT enabled watch kept on it, start charging it and will stop charging when watch is removed from it. For watches with 3.6 V batteries, it can detect charge completion and stop charging. For all other battery levels it will automatically stop charging after 5 hours. It can also detect the type of battery inside the charger and charge it accordingly.

The maximum efficiency of 35.2% was achieved for a load current of 45 mA. As the load current reduces, the efficiency decreases. The efficiency comes down to less than 5% when charging the low capacity batteries which has a charging current of 2 mA or less.

A patent application is filed for the developed system titled “An apparatus and method for wireless detection of wristwatch with conductive back plate and wireless charging of its battery”, patent No. 1507/CHE/2014.

5.2 Future Scope

During the charging process, the charging current reduces as the battery charge level increases. As the load current reduces, primary coil current and hence the magnetic field produced by it increases thereby increasing the heating. A system based on sensing the primary current and reducing it by increasing the switching frequency can be developed to reduce this heating.

A charge completion detection system for the lower voltage batteries by sensing its voltage using a voltage detector IC and using its output to change the tuning of the secondary can also be tried. The next step towards improving the user convenience would be to try for better positional tolerance for the watch on the charger.

APPENDIX A

PCB LAYOUTS

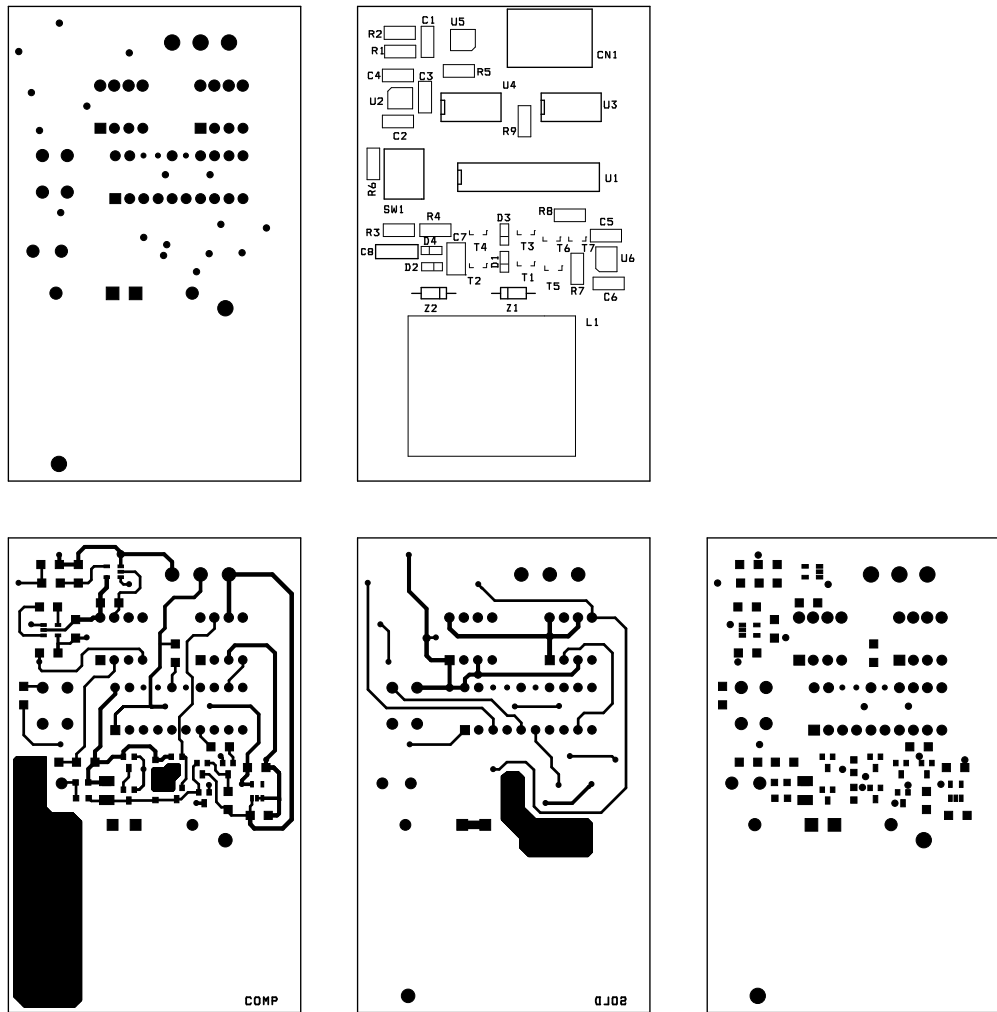
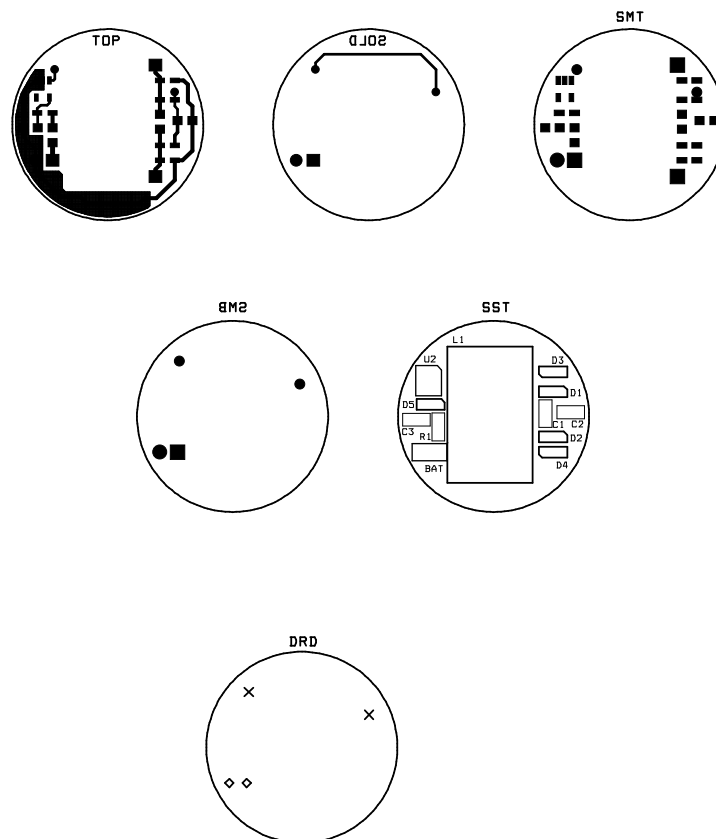


Figure A.1: Transmitter PCB layout



DRILL CHART				
SYM	DIAM	TOL	QTY	NOTE
x	0.500 mm		2	
o	0.900 mm		2	
TOTAL			4	

Figure A.2: Receiver PCB layout

REFERENCES

- [1] N. Tesla, “Apparatus for transmitting electrical energy,” Patent US 1 119 732, Dec 1, 1914.
- [2] D. Schneider, “Electrons unplugged,” *IEEE Spectr.*, vol. 47, no. 5, pp. 34–39, May 2010. [Online]. Available: <http://dx.doi.org/10.1109/MSPEC.2010.5453139>
- [3] A. Partovi, “Systems and methods for wireless power transfer,” Patent US 0 285 604, Oct 31, 2013.
- [4] G. A. Covic and M. L. G. Kissin, “Inductive power receiver circuit,” Patent US 0 285 463, Oct 31, 2013.
- [5] T. Toivola and J. O. Hautala, “Wireless battery charging system,” Patent US 0 194 124, Aug 2, 2012.
- [6] H. J. Brockmann and Heikki, “Charger with inductive power transmission for batteries in a mobile electrical device,” Patent US 0 194 124, Aug 2, 2012.
- [7] H. Zangl, A. Fuchs, T. Bretterklieber, M. Moser, and G. Holler, “Wireless communication and power supply strategy for sensor applications within closed metal walls,” *Instrumentation and Measurement, IEEE Transactions on*, vol. 59, no. 6, pp. 1686–1692, June 2010.
- [8] “Nokia lumia 920,” <http://www.nokia.com> , 2014.
- [9] “Ti bqtesla wireless power transmitter and receiver,” <http://www.ti.com> , 2014.
- [10] X. Liu, W. M. Ng, C. Lee, and S. Hui, “Optimal operation of contactless transformers with resonance in secondary circuits,” in *Applied Power Electronics Conference and Exposition, 2008. APEC 2008. Twenty-Third Annual IEEE*, Feb 2008, pp. 645–650.
- [11] C.-S. Wang, G. Covic, and O. Stielau, “Power transfer capability and bifurcation phenomena of loosely coupled inductive power transfer systems,” *Industrial Electronics, IEEE Transactions on*, vol. 51, no. 1, pp. 148–157, Feb 2004.
- [12] “Panasonic battery charging specification manual,” <http://www.panasonic-batteries.com> , 2014.

CURRICULUM VITAE

Name : Anish Babu
Date of Birth : 18 May, 1987
Place of Birth : Kottayam, Kerala
Education : B.Tech from National Institute of Technology, Calicut
Work Experience : Consulting Engineer, KalkiTech
E-mail : anishb87@gmail.com
Publications : Patent Filed: Anish Babu, Bobby George, Srivalli S.P, “An apparatus and method for wireless detection of wristwatch with conductive back plate and wireless charging of its battery”,
Patent No: 1507/CHE/2014.